A New Reference Correlation for the Viscosity of Methanol

Hong Wei Xiang,[a] Arno Laesecke, and Marcia L. Huber[b]

Physical and Chemical Properties Division, National Institute of Standards and Technology, Boulder, Colorado 80305

(Received 24 March 2004; revised manuscript received 4 September 2006; accepted 10 September 2006; published online 8 November 2006)

A new reference-quality correlation for the viscosity of methanol is presented that is valid over the entire fluid region, including vapor, liquid, and metastable phases. To describe the zero-density viscosity with kinetic theory for polar gases, a new expression for the collision integral of the Stockmayer potential is introduced. The initial density dependence is based on the Rainwater–Friend theory. A new correlation for the third viscosity virial coefficient is developed from experimental data and applied to methanol. The high-density contribution to the viscosity is based on the Chapman–Enskog theory and includes a new expression for the hard-sphere diameter that is a function of both temperature and density. The resulting correlation is applicable for temperatures from the triple point to 630 K at pressures up to 8 GPa. The estimated uncertainty of the resulting correlation (with a coverage factor of 2) varies from 0.6% in the dilute-gas phase between room temperature and 630 K, to less than 2% for the liquid phase at pressures up to 30 MPa at temperatures between 273 and 343 K, 3% for pressures from 30 to 100 MPa, 5% for the liquid from 100 to 500 MPa, and 10% between 500 MPa and 4 GPa. At very high pressures, from 4 to 8 GPa, the correlation has an estimated uncertainty of 30% and can be used to indicate qualitative behavior. [DOI: 10.1063/1.2360605]

Key words: Chapman–Enskog theory; collision integral; hard-sphere diameter; high pressure; Lennard-Jones potential; methanol; polarity; Rainwater–Friend theory; Stockmayer potential; third viscosity virial coefficient; transport properties; viscosity.

CONTENTS

List of Tables

List of Figures

[a]Permanent address: Institute of Chemistry, Chinese Academy of Sciences, Zhongguancun, Haidian, Beijing 100080, China.
[b]Author to whom correspondence should be addressed. Electronic mail: marcia.huber@NIST.gov

1. Introduction

Methanol (CH_3–OH) is a widely used fluid in the chemical and process industries. It is also an important compound for healthcare as well as medical and pharmaceutical applications. The oldest use of methanol is in the conversion of biomass. This process is gaining importance because it produces a fuel that does not cause a net increase of carbon dioxide in the Earth's atmosphere. Even more prominent is the role of methanol as a hydrogen-rich fuel for electrochemical energy converters such as fuel cells.[22] In fact, the future hydrogen economy may largely rely on methanol because it is safer to distribute hydrogen chemically bonded in liquid form than as a pure compound through gas pipelines. Some other applications of methanol include heat pipes in solar energy applications,[68] working fluid in cooling microelectronics,[79] and as an inhibitor of the formation of gas hydrates in pipelines.[69] The development of accurate thermophysical property formulations for methanol will aid engineers involved in process design in these and other fields. In addition, since it is the first member of the homologous series of alkanols, its physical properties will help to characterize the properties of the series as a whole.[27,58] Although a reference-quality equation of state has been developed for the thermodynamic properties of methanol,[28] a comprehensive study of the viscosity of methanol has not yet been carried out. This work fills this gap by selecting the most reliable measurements as the basis for a new reference correlation for the viscosity of methanol that is valid over the entire fluid region for vapor, liquid, and supercritical states.

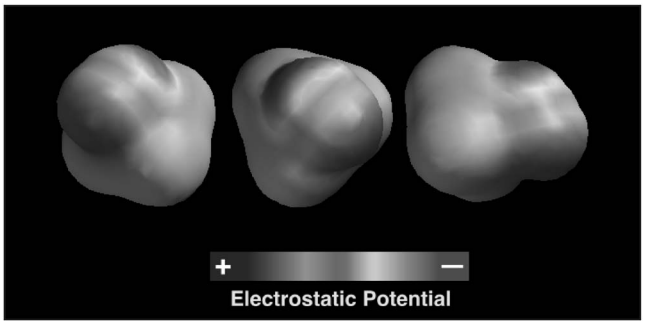

FIG. 1. Visualization of the methanol molecule in terms of the isoelectron density surface 0.22×10^{10} C m^{-3} with the electrostatic potential indicating the charge distribution/polarity. The molecule is shown in three orientations to give a better impression of its size, shape, charge distribution, and polar centers.

There are a number of approaches that have been used to model the viscosity of a fluid over a wide range of conditions including the friction theory model,[106,107] free-volume and friction models,[1,2,13] other free-volume models,[63,136] as well as completely empirical correlations.[96] We take a different approach here, and use an advanced residual concept for the correlation of the viscosity. In this approach, the viscosity of a fluid is expressed as a function of density and temperature and contains a zero-density limit term, a linear-in-density term, and a third virial coefficient for the quadratic density term, and higher-density terms for the compressed fluid region. The objective of this work is to apply kinetic theory to the dilute gas, Rainwater–Friend theory, and the third viscosity virial coefficient for the moderately dense gas, and the Enskog dense hard-sphere theory to obtain a correlation for the viscosity of methanol for the entire fluid state that reproduces the most reliable data sets to within their estimated uncertainties and describes the phenomenological behavior of the viscosity of methanol from the triple point to 630 K at pressures up to 8 GPa.

2. Molecular Structure

Methanol is one of the most polar molecules, and its size, shape, and charge distribution determine its macroscopic properties. Among these, viscosity is most sensitive to molecular interactions as it varies over 23 orders of magnitude from the least viscous gas to the most viscous solid.[75] Molecular features should be accounted for as much as possible to reduce empiricism and to extend the applicability of representative property formulations beyond the range of experimental data. The size, shape, and charge distribution of methanol are illustrated in Fig. 1 in terms of an iso-surface of

TABLE 1. Critical temperatures, molecular surface areas, and molecular volumes of methanol, carbon dioxide, and ethane

Chemical name	T_c (K)	$A/(10^{-20}\ m^2)$	$V/(10^{-30}\ m^3)$
Methanol	512.6	62.17	41.80
Carbon dioxide	304.1282	56.07	36.02
Ethane	305.33	73.06	52.35

the electron density at 0.22×10^{10} C m^{-3} ($0.002\ e^-$ bohr^{-3}) with the electrostatic potential mapped onto it.[45] This electron density level represents about 98% of a molecule. The isoelectron density surface and the charge distribution were calculated *ab initio* in the Hartree–Fock approximation using the 6-31G* basis set.[59] The unique interactions between methanol molecules become evident by comparing its molecular surface area A, volume V, and critical temperature T_c with those of similar molecules. Carbon dioxide (CO_2) and ethane (C_2H_6) are chosen for this comparison because they are quadrupolar or nonpolar, with a more homogeneous charge distribution than methanol, while their molecular surface areas and volumes, calculated in the same approach as mentioned above, bracket those of methanol. The values are compiled in Table 1. While the critical temperatures of carbon dioxide and ethane scale with their molecular surface areas and volumes, the critical temperature of methanol exceeds both by more than 200 K. Thus, the attractive forces among methanol molecules are considerably stronger than among the other two molecules.

These higher attractive forces in methanol arise primarily from the polarity of the molecule, but their effect depends also on the molecular architecture. In systems of small molecules, the long-range electrostatic attractions lead to the formation of associates that are favored when the molecules can interlink easily due to their geometry. These associations are strongest in small molecules with highly separated charges, e.g., hydrogen fluoride. The existence of hydrogen bonds in methanol is well known, but their effect is not as strong as in hydrogen fluoride or water. Given these microscopic features of methanol, a correlation of its viscosity should account for the asphericity of the molecule, for long-range electrostatic attractions due to its polarity, and for the formation of associates under certain conditions. Clearly, a theoretical framework to incorporate all these interactions in wide-ranging correlations has yet to be developed. Nevertheless, the viscosity correlation in this work includes as much theory as possible.

3. Equation of State

An equation of state is essential for the correlation of viscosity, since experimental data are generally measured in terms of pressure and temperature, while theory suggests considering the viscosity in terms of density and temperature. In this work, we calculate the density from the equation of state for methanol by de Reuck and Craven.[28] It has an uncertainty of 0.1%–0.2% in density in the vapor phase up to approximately 1 MPa and in the liquid phase up to about 250 MPa. Slightly larger uncertainties apply in the vicinity of the critical point. For further details on the equation of state and its uncertainties, we refer the reader to the IUPAC monograph of de Reuck and Craven.[28] For pressures above 1 GPa, instead of using the equation of state of de Reuck and Craven,[28] we use a Tait equation given by Cook *et al.*[24] that is based upon the measurements of Bridgman.[15,16] We found better correlation of the data using these densities than with densities interpolated from the more recent density measurements up to 30 GPa obtained by Zaug *et al.*[145] There is a need for further experimental work to resolve discrepancies in density measurements at very high pressures.

4. Experimental Viscosity Data

A number of compilations of the viscosity of methanol have been carried out before but none of them was entirely inclusive. Bingham *et al.*[11] in 1913 compared their results with data from eight previous publications. Timmermans and Hennaut-Roland[124] noted that the viscosity of methanol had been the subject of numerous studies but referenced only five of them. In 1973 Zubarev *et al.*[147] correlated data from 13 literature sources dating from 1930 to 1968. These formed the basis of the tables in the second edition (1975) of the handbook of Vargaftik *et al.*[132] and they were republished unchanged in the third edition of 1996. In 1975, Touloukian *et al.*[127] provided recommended values for the viscosity of gaseous methanol in the temperature range 250–650 K from an evaluation of five literature data sources from 1933 to 1960. Yaws[143] reported correlations for the viscosity–temperature dependence of the vapor and the liquid at atmospheric pressure referring only to previous compilations but not to original experimental data. In 1979 Stephan and Lucas[119] generated tables and plots of the viscosity of liquid methanol as a function of temperature and pressure covering 290–550 K with pressures to 80 MPa, based upon the data of Golubev and Petrov[47] (as reported in Golubev[48]) and those of Isakova and Oshueva.[66] They also used the compilation of Touloukian *et al.*[127] and the 1960 edition of the Landolt–Börnstein tables. Liley *et al.*[82] generated viscosity data tables of both the liquid and vapor phases relying heavily upon the work of Stephan and Lucas.[119] Viswanath and Natarajan[134] reported a viscosity–temperature correlation for the liquid at atmospheric pressure based on only three literature data sets. The German national metrology institute Physikalisch-Technische Bundesanstalt (PTB) published in the early 1990s a series of recommended property values for various compounds. The issue on methanol appeared in 1993 and contained a viscosity–temperature correlation for the saturated liquid from 183 to 415 K based on ten sources of original experimental data from 1958 to 1993. Barthel *et al.*[9] considered a total of 64 publications and included data of 41 of them in a viscosity–temperature correlation for liquid methanol from 223 to 328 K. In addition to cross-checking all previously mentioned compilations and original data sources, a comprehensive literature survey in the computer databases NIST TRC SOURCE,[42] DIPPR DIADEM,[113] and

the Landolt–Börnstein data collection (Wohlfarth and Wohlfarth[142]) was performed. This resulted in a total of 243 literature sources of original experimental results or compiled and evaluated data for the viscosity of methanol from 1861 to 2006. With this many investigations, methanol is after water and ethanol the third most measured fluid in viscometry. A detailed documentation and discussion of this body of data is beyond the scope of this paper and will be published separately. Here, we confine ourselves primarily to a discussion of those data that were used in the development of the wide-ranging correlation.

The first viscosity measurements for methanol were performed in 1861 by Graham[52] in the liquid phase at atmospheric pressure. A number of such studies followed until Bridgman[14] in his pioneering work performed the first measurements on compressed methanol with a falling-body viscometer. Later Bridgman[17] extended the range to 3 GPa and 100 mPa s using a swinging-vane apparatus. Herbst *et al.*[60] determined the viscosity of methanol in the same pressure range as Bridgman[17] by means of dynamic light scattering measurements in a diamond anvil cell, and Cook *et al.*[24] extended the pressure range to 8.35 GPa with the centrifugal force rolling-sphere/diamond anvil cell viscometer. Note that most of their results pertain to the supercompressed liquid because the freezing pressure of methanol at 297 K is approximately 2.6 GPa [see Fig. 2(a)]. The most recent high-pressure investigation of this type is that of Grocholski and Jeanloz[54] to 6.5 GPa in the temperature range 298–338 K also including several state points in the supercompressed liquid region above the melting pressure curve. Harlow[57] and Isdale *et al.*[67] measured the viscosity of methanol also near room temperature to pressures of 935 and 472 MPa, respectively. Their results agree mutually within their experimental uncertainties; however the uncertainties are considerably higher than at lower pressures.

An important investigation was carried out by Mitsukuri and Tonomura[92] in 1927, who measured the viscosity of liquid methanol from room temperature down to the triple point. These data were republished by Tonomura.[126] They agree quite well with the more recent measurements of Golubev and Potikhonova,[50] of Yergovich *et al.*,[144] and of Schneider[114] in the overlapping range of low temperatures at atmospheric pressure. Titani[125] in 1933 was the first to measure the viscosity of gaseous methanol, substantially extending the temperature range to 585 K. Blokker[12] followed with high-temperature viscosity measurements of saturated liquid methanol from room temperature up to 491 K. His results agree well with subsequent measurements as seen in Table 2. Within this range of temperature, Isakova and Oshueva[66] measured the viscosity of methanol from room temperature to 433 K at pressures up to 24.5 MPa, including four points in the metastable liquid region at atmospheric pressure and temperatures of 353, 373, 393, and 413 K. This dataset overlaps with the measurements of Weber[138] at PTB from room temperature to 373 K with pressures to 49.1 MPa. In addition, two other data sets obtained by Kubota *et al.*[77] and by Tanaka *et al.*[121] are from room temperature to 348 K at pressures to 68.8 MPa. To extend previous measurements to higher temperatures, Golubev and Petrov[47] measured the viscosity of methanol from 423 to 543 K at pressures up to 81 MPa. The measurements of Golubev and Likachev[51] ranged from 296 to 674 K with pressures to 50 MPa in the compressed liquid region and in the subcritical gas phase. Their supercritical measurements reached the highest temperature of viscosity measurements on methanol to date. In the dilute gas phase, Vogel and collaborators[122,135] have made extensive measurements with an oscillating disk apparatus at temperatures up to 615 K.

This brief review discusses only the more comprehensive data sets for the viscosity of methanol. Table 2 gives a more detailed data compilation including experimental methods, temperature and pressure ranges, phase state, number of reported data points, and reported or ascribed uncertainty. Several criteria, including sample purity and uncertainty level are used to select the primary data (shown in bold type in Table 2) and preference is also given to data sets that cover a wide range of temperature and pressure. The distribution of the available experimental viscosity data for methanol is illustrated in the pressure–temperature diagram in Fig. 2(a). Relevant for the correlating formulation is the viscosity–density dependence, which is shown in Fig. 2(b). The temperatures associated with all viscosity data were converted to the ITS-90 temperature scale.[105]

5. Methodology

The understanding of the viscosity has not yet progressed to the level where a theory of molecular interactions would allow the macroscopic transport property over wide ranges of the fluid region to be calculated in a consistent fashion. However, such an understanding has evolved in subdomains of the fluid region such as the low-density gas and the liquid. The present correlation of the viscosity of methanol is a synthesis of these theoretically well understood molecular interaction mechanisms. The viscosity η as a function of temperature T and density ρ is due to two contributions:

$$\eta(\rho,T) = f \cdot \eta_g(\rho,T) + (1-f) \cdot \eta_E(\rho,T). \quad (1)$$

The viscosity at low densities is described by kinetic theory as a virial expansion in density

$$\eta_g(\rho,T) = \eta^\circ(T)[1 + B_\eta(T) \cdot \rho + C_\eta(T) \cdot \rho^2 + \ldots], \quad (2)$$

with the viscosity in the limit of zero density $\eta^\circ(T)$. The expansion is truncated after the quadratic term and a logarithmic term is not taken into account. $B_\eta(T)$ and $C_\eta(T)$ are the second and third viscosity virial coefficients. The contribution to the viscosity representing interactions under liquid conditions, $\eta_E(\rho,T)$, is adopted from Enskog's theory for hard spheres.[23,33,34] Instead of simply adding them, we combine these contributions by a transition or crossover function

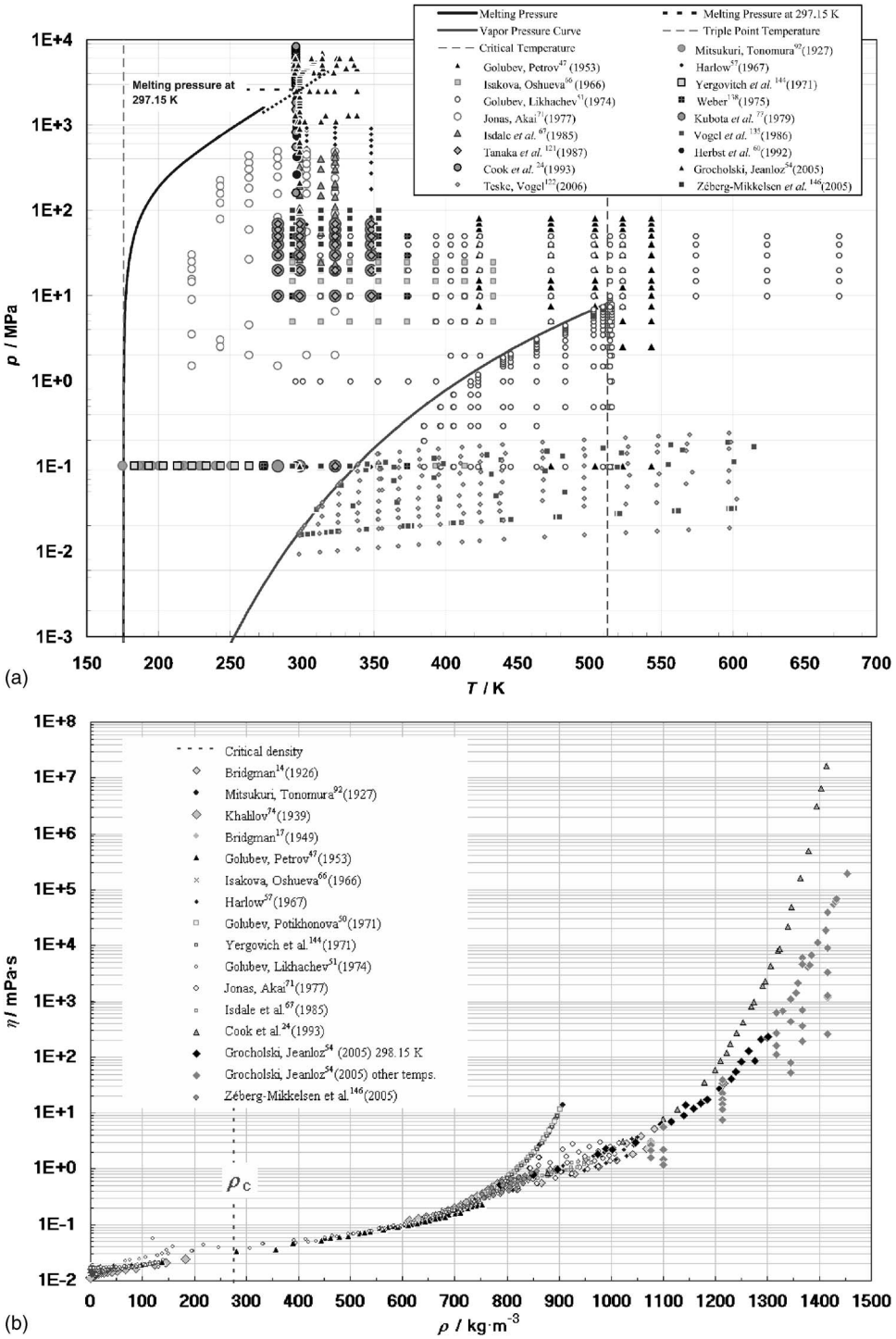

FIG. 2. (a) Pressure–temperature coverage of the available experimental viscosity data for methanol and (b) density dependence of the viscosity data of methanol.

f, treated in more detail in Sec. 5.4, which reflects the gradual transition from one mechanism of molecular interaction to another. Details of the contributions to the viscosity are discussed below.

5.1. Viscosity in the Zero-density Limit

The viscosity η° of a fluid in the limit of zero density is not directly accessible experimentally. It is generally determined by extrapolating available experimental data at low densities to zero density. The theoretical models for gas or vapor-phase viscosity are based on kinetic theory. According to the rigorous kinetic theory of gases,[62] the viscosity η° of a dilute gas of spherical particles is given by

$$\eta^\circ = 5\sqrt{mkT/\pi}/(16\sigma_0^2\Omega^{(2,2)^*}), \tag{3}$$

where $k = 1.380\,6505 \times 10^{-23}$ K^{-1} is the Boltzmann constant,[93] $m = M/N_A$ is the molecular mass with M being the molar mass, and $N_A = 6.022\,1415 \times 10^{23}$ mol^{-1} is Avogadro's constant.[93] The collision diameter σ_0 is defined as the smallest separation distance where the intermolecular

TABLE 2. List of selected experimental data of the viscosity of methanol and percent deviations from the present method, Eq. (18). Authors whose data were used in the correlation are printed in bold. Data sets with fewer than three data points are not listed

Author	Year	Instrument, Method	Reported uncertainty	Temperature range, (K)	Pressure range (MPa)	No. of points	AAD (%)	Bias (%)	RMS (%)	Max. dev. (%)
Thorpe, Rodger[123]	1894	Open gravitational capillary	Not reported	277–336	Atmospheric	13	1.6	1.6	0.79	3.4
Getman[44]	1906	Ostwald capillary flow	Not reported	283–313	Atmospheric	7	1.4	1.4	0.60	2.2
Tower[128]	1916	Mod. Bingham viscometer	Not reported	289–313	Atmospheric	3	1.2	0.45	1.14	1.5
Bridgman[14]	1926	Falling body	Not reported	303–348	0.1–1176	18	4	−0.81	5	−13
Mitsukuri, Tonomura[92]	1927	Ostwald capillary flow	Not reported	175–273	Atmospheric	13	1.5	−0.26	1.9	4.7
Herz, Levi[61]	1929	Ostwald capillary flow	Not reported	293–323	Atmospheric	4	1.7	1.7	1.1	3.1
Hughes, Hartley[64]	1933	not reported	not reported	298	Atmospheric	1	0.22	0.22	0	0.22
Titani[125]	1933	Const. flow rate capillary	Not reported	384–585	Atmospheric, saturation	7	0.76	0.65	0.61	1.3
Blokker[12]	1936	Gravit. capillary flow	1%	298–491	Atmospheric	16	3.0	1.41	3.1	6
Khalilov[74]	1939	Gravit. capillary flow	Not reported	293–443	Sat. liq and vapor	38	4.1	2.8	3.9	11
Amis *et al.*[6]	1942	Ostwald capillary flow	1.6%	283–323	Atmospheric	5	0.45	0.18	0.48	0.74
Grant *et al.*[53]	1948	Gravit. capillary flow	Not reported	273–333	Atmospheric	8	0.82	0.67	0.54	1.30
Bridgman[17]	1949	Swinging vane		298	490–2941	6	9.8	9.8	3.9	17
Fischer[35]	1949	Ubbelohde capillary flow	Not reported	293–313	Atmospheric	4	2.4	2.4	1.1	4
Craven, Lambert[26]	1951	Swinging pendulum	1%	308–350	Dilute gas	4	1.4	1.4	0.24	1.6
Golubev, Petrov[47]	1953,70	Forced capillary flow	1%	423–543	0.1–81	66	1.90	−0.05	3.2	−18
Richardson[112]	1954	Literature data?	Not reported	283–313	Atmospheric	4	0.93	0.93	0.54	1.8
Foster, Amis[38,39]	1955,56	Ostwald capillary flow	Not reported	298–318	Atmospheric	3	0.88	0.88	0.51	1.5
Golik *et al.*[46]	1955	Capillary flow?	Not reported	293–413	Atmospheric	13	3.33	2.30	3.04	6.05
Sears *et al.*[115]	1955	Ostwald-Cannon-Fenske	Not reported	223–298	Atmospheric	9	2.0	−2.0	1.1	−3.23
Ledneva[80]	1956	Literature data?	Not reported	293.15–443.15	Saturation	16	3.3	2.5	2.9	6.3
Whorton, Amis[140]	1956	Ostwald capillary flow	Not reported	298–318	Atmospheric	3	0.28	0.28	0.20	0.53
Hammond *et al.*[56]	1958	Cannon-Ubbelohde capillary flow	0.2%	293–338	Atmospheric	6	0.50	0.36	0.43	0.93
Ling, van Winkle[84]	1958	Cannon-Fenske capillary flow	0.2% (liq.) 4% (vap.)	303–423	Atmospheric, saturation	6	3.3	3.3	23	5.8
Uchida, Matsumoto[130]	1958	Ostwald capillary flow	Not reported	303–333	Atmospheric	6	2.9	2.9	0.87	4.0
Mikhail, Kimel[91]	1961	Cannon-Fenske capillary flow	Not reported	298–323	Atmospheric	5	16	−16	13	−38
Lindberg[83]	1962	Ostwald capillary flow	0.3%	298–319	Atmospheric	3	0.55	−0.41	0.44	0.74
Bamelis *et al.*[8]	1965	Ostwald capillary flow	Not reported	298–328	Atmospheric	4	0.49	0.49	0.26	0.76
Isakova, Oshueva[66]	1966	Forced capillary flow	1%	293–433	0.1–24.5	47	2.4	−1.7	2.7	−6.7
Harlow[57]	1967	Falling cylinder	1.4%	303–348	0.1–935	32	2.5	2	2.8	8.4
Pal, Barua[101]	1968	Oscillating disk	0.5%	303–477	Dilute gas	5	4.8	−4.8	1.43	−7.5
Mato, Hernandez[86]	1969	Falling sphere	0.2%	288–323	Atmospheric	7	3.6	1.3	4.2	−7.6
Konobeev, Lyapin[76]	1970	Pinkevich capillary flow	Not reported	293–333	Atmospheric	3	0.90	0.17	0.90	−1.1
Golubev, Kovarskaya[49]	1971	Forced capillary flow	1.0%	373, 473, 573	Atmospheric	3	1.0	1.0	0.31	1.3
Golubev, Potikhonova[50]	1971	Forced capillary flow	1.5%	178–338	Atmospheric	33	1.1	0.11	1.30	−2.6
Mato, Coca[87]	1971	Höppler rolling sphere	Not reported	298–328	Atmospheric	3	1.1	−1.1	0.67	−2.0
Yergovich *et al.*[144]	1971	Cannon-Fenske capillary	1.9%	183–283	Atmospheric	11	3	−3	1.2	−4.5
Golubev, Likhachev[51]	1974	Forced capillary flow (5th variant)	1.0%	295.35–673.95	0.1–50	350	2.1	1.2	4.3	41
Janelli *et al.*[70]	1974	Ubbelohde capillary flow	Not reported	303–313	Atmospheric	3	0.44	0.44	0.16	0.63
Touloukian *et al.*[127]	1975	Compilation	1%	250–650	Atmospheric	41		Not compared		
Weber[138]	1975	Ubbelohde capillary flow, Höppler rolling sphere	0.3% at low T to 1.5%	273–373	0.1–49.1	17	1.1	−0.92	1.00	−3.0
Lee[81]	1976	Cannon-Fenske capillary	Not reported	288–323	Atmospheric	6	0.56	0.56	0.33	1.2
Jonas, Akai[71a]	1977	Rolling sphere	3%	223–323	1.5–490.5	43	3.4	0.88	4.0	−8.9
Medani, Hasan[89]	1977	Rolling sphere	Not reported	353–463	Atmospheric	12	18	−18	12	−40
Schneider[114b]	1978	Forced capillary flow	Not reported	184–313	Sat. liq.	27	2.2	0.47	3.4	−14
Kubota *et al.*[77]	1979	Falling cylinder	2%	283–348	0.1–68.8	31	1.6	0.33	1.80	−3.8
Stephan, Lucas[119]	1979	Compilation	6%	290–550	0.1–80	210		Not compared		
Werblan[139]	1979	Ubbelohde capillary flow	0.13 μPa s	298	Atmospheric	4	2.6	2.6	0.76	3.9
Dizechi, Marschall[29]	1982	Ubbelohde capillary flow	Not reported	283–323	Atmospheric	5	1.2	1.2	0.59	1.7
Rauf *et al.*[110]	1983	Ubbelohde capillary flow	Not reported	288–328	Atmospheric	5	0.89	0.82	0.73	1.9
Doe *et al.*[31]	1984	Ostwald capillary flow	Not reported	278–318	Atmospheric	5	0.95	−0.45	1.0	−2.1
Martin *et al.*[85]	1984	Ostwald-Cannon-Fenske capillary flow	Not reported	298–323	Atmospheric	4	1.21	−0.11	1.4	−2
Doe, Kitagawa[32]	1985	Ostwald capillary flow	Not reported	278–318	Atmospheric	5	0.95	−0.45	1.1	−2.1
Isdale *et al.*[67]	1985	Falling body	2%	298–323	0.1–472	44	2.8	−2.3	3.0	−11
Vogel *et al.*[135]	1986	Oscillating Disk	0.3%	301–615	Dilute Gas	60	0.14	−0.09	0.19	−0.69
Tanaka *et al.*[121]	1987	Falling cylinder	2%	283–348	0.1–68.8	31	1.5	0.32	1.7	−3.5

TABLE 2. List of selected experimental data of the viscosity of methanol and percent deviations from the present method, Eq. (18). Authors whose data were used in the correlation are printed in bold. Data sets with fewer than three data points are not listed—Continued

Author	Year	Instrument, Method	Reported uncertainty	Temperature range, (K)	Pressure range (MPa)	No. of points	AAD (%)	Bias (%)	RMS (%)	Max. dev. (%)
Liley *et al.*[82]	1988	Compilation	6%–10%	290–550 (Sat. Liq.: T_b–T_c)	0.1–80			Not compared		
Viswanath, Natarjan[134]	1989	Compilation, Correlation	Not applicable	180–293	Atmospheric			Not compared		
Joshi *et al.*[72]	1990	Cannon-Fenske	0.7 μPa s	298–313	Atmospheric	5	1.7	−0.21	2.1	−3.4
Soliman, Marschall[118]	1990	Ubbelohde capillary flow	0.3%	283–323	Atmospheric	6	1.2	1.2	0.65	1.9
Crabtree, O'Brien[25]	1991	Ubbelohde capillary flow	Not reported	303–319	Atmospheric	3	0.96	0.96	0.29	1.3
Garcia *et al.*[43]	1991	Cannon-Fenske capillary	Not reported	298–323	Atmospheric	4	0.28	0.08	0.31	−0.41
Joshi *et al.*[73]	1991	Cannon-Fenske capillary	0.7 μPa s	298–313	Atmospheric	4	2.4	−1.9	1.7	−3.4
Matsuo, Makita[88]	1991	Forced capillary flow	2%	303–323	0.1–30	24	0.74	−0.24	0.79	−1.3
Herbst *et al.*[60]	1992	Dynamic light scattering	5.8%	297	0.1–2900	12	12	11	8.9	25
Papanastasiou, Ziogas[104]	1992	Ubbelohde capillary flow	0.17%	288–308	Atmospheric	5	0.66	−0.66	0.19	−0.89
Aminabhavi *et al.*[3]	1993	Cannon-Fenske capillary	0.2%	298–308	Atmospheric	3	0.24	−0.00	0.27	0.35
Cook *et al.*[24]	1993	Centrifugally accelerated rolling sphere	2.8%–12%	296	0.1–8350	27	14	−0.35	17	43
Dobberstein *et al.*[30]	1993	Ubbelohde capillary flow	10^{-9} m^2 s^{-1}	293–318	Atmospheric	6	0.61	0.61	0.34	1.02
Papaioannou *et al.*[102]	1993	Falling body	2.5%	298	0.1–71.7	11	2.3	−2.2	1.4	−4.2
Assael, Polimatidou[7]	1994	Vibrating wire	0.5%	290–340	0.1–30	26	0.73	0.31	0.79	1.50
Papaioannou, Panayiotou[103]	1995	Falling body	2.5%	298	0.1–51.8	12	2.3	−23	1.3	−3.8
Muhuri *et al.*[95]	1996	Ubbelohde capillary flow	0.2%	298–318	Atmospheric	3	1.2	1.2	0.82	1.9
Nikam *et al.*[99]	1996	Ostwald capillary flow	1 μPa s	298–303	Atmospheric	2	2.8	2.8	0.41	3.2
Nikam *et al.*[100]	1996	Ostwald capillary flow	1 μPa s	298–308	Atmospheric	3	2.9	2.9	1.2	4.2
Vargaftik *et al.*[133]	1996	Compilation	Not applicable	178–573	0.1–50			Not compared		
Barthel *et al.*[9]	1997	Compilation, Correlation	Not applicable	223–328	Atmospheric			Not compared		
Aminabhavi, Patil[5]	1998	Cannon-Fenske capillary flow	1 μPa s	298–308	Atmospheric	3	0.73	−0.73	0.24	−1.1
Aminabhavi, Banerjee[4]	1998	Ubbelohde capillary flow	1 μPa s	298–308	Atmospheric	3	7.3	−7.3	0.24	−7.7
Kumagai, Yokoyama[78]	1998	Sealed gravitat. capillary	1.3%	273–333	Atmospheric	4	1.1	0.16	1.10	−1.4
Nikam *et al.*[100]	1998	Ubbelohde capillary flow	0.1%	298–313	Atmospheric	4	2	2	0.22	2.3
Landolt-Börnstein (Wohlfarth, Wohlfarth)[142]	2001	Compilation	Not applicable	Various	Various			Comparison with original data		
Tu *et al.*[129]	2001	Ubbelohde capillary flow	0.7%	293–313	Atmospheric	4	0.86	0.86	0.47	1.4
Grocholski, Jeanloz[54]	2005	Centrifugally accelerated rolling sphere	9%–28%	298–338	1100–6050	79	42.9	17.8	57.8	99.6
Zéberg-Mikkelsen *et al.*[146]	2005	Falling body	2%	293–353	0.1–100	23	1.0	−0.22	1.3	−2.8
Teske, Vogel[122]	2006	Oscillating disk	0.2%–0.3%	298–598	Dilute gas	169	0.18	0.06	0.31	2

[a]Deuterated methanol.
[b]Only 16 points used in primary set.

potential function is equal to zero, and $\Omega^{(2,2)*}$ is a collision integral that depends upon the potential function. For nonpolar gases, the Lennard-Jones potential is often applied. Neufeld *et al.*[98] developed empirical correlations for the temperature dependencies of the transport collision integrals of the Lennard-Jones 12-6 potential, which represent $\Omega^{(2,2)*}$ in terms of the reduced temperature $T^*=kT/\varepsilon_0$ in the range $0.3 \leqslant T^* \leqslant 100$ with an uncertainty of 0.1%. Here, ε_0 is the depth of the minimum of the interaction potential between two particles. The correlation of Neufeld *et al.*[98] for the collision integral $\Omega^{(2,2)*}$ is without the sine terms

$$\Omega_{\mathrm{LJ}}^{(2,2)^*} = a_0(T^*)^{a_1} + a_2 e^{a_3 T^*} + a_4 e^{a_5 T^*}. \tag{4}$$

The subscript LJ refers to the Lennard-Jones potential. For polar gases, application of the Stockmayer (12-6-3) potential $\varphi_{\mathrm{SM}}(r)$

$$\varphi_{\mathrm{SM}}(r) = 4\varepsilon_0[(\sigma_0/r)^{12} - (\sigma_0/r)^6 + \delta(\sigma_0/r)^3], \tag{5}$$

$$\delta = (1/4)\mu^{*2}\zeta, \quad \mu^{*2} = \mu/(\varepsilon_0\sigma_0^3)^{1/2}, \tag{6}$$

$$\zeta = (1/2)[2\cos\theta_a\theta_b - \sin\theta_a \sin\theta_b \cos\psi], \tag{7}$$

is more appropriate, since it includes a parameter δ that accounts for the anisotropic charge distribution from which the polarity of a particle characterized by the dipole moment μ arises (Hirschfelder *et al.*[62]). θ_a and θ_b are the angles of inclination of the dipole axis to the line joining the centers of two molecules, ψ is the azimuthal angle between them, and r is the separation distance. This potential function represents the molecular interactions by adding an embedded point dipole vector to a Lennard-Jones potential, and it reduces to the Lennard-Jones 12-6 potential when the dipole moment is zero. Monchick and Mason[94] presented the values of the reduced orientation-averaged collision integral $\Omega_{\mathrm{SM}}^{(2,2)*}$ calculated from the Stockmayer (12-6-3) potential in the range of $0.1 \leqslant T^* \leqslant 100$ and $0 \leqslant \delta \leqslant 2.5$. Figure 3 shows the collision integral $\Omega_{\mathrm{SM}}^{(2,2)*}$ as a function of the inverse reduced tempera-

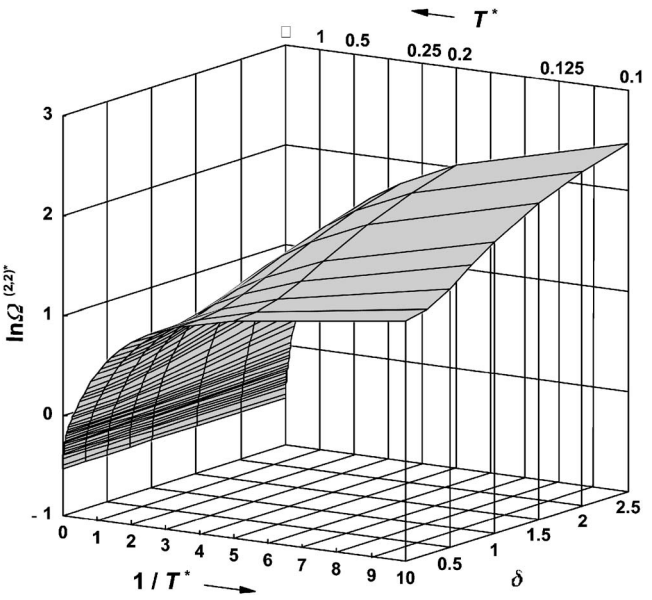

FIG. 3. The collision integral $\Omega^{(2,2)^*}$ of the Stockmayer potential as a function of inverse reduced temperature $1/T^*$ and polarity parameter δ.

ture $1/T^*$ and the reduced dipole moment δ. It is desirable to have a convenient expression similar to that developed by Neufeld *et al.*[98] for the Lennard-Jones 12-6 potential to facilitate calculations. Brokaw[18] developed a simple approximation for $\Omega_{SM}^{(2,2)*}$, where $\Omega_{SM}^{(2,2)*}=\Omega_{LJ}^{(2,2)*}+0.2\delta^2/T^*$. This expression reproduced the values of Monchick and Mason[94] with an average absolute deviation of 1.6%, a maximum deviation of 19%, and a standard deviation of 2.7% over the temperature range $0.3\leqslant T^*\leqslant 100$ and $0\leqslant\delta\leqslant 2.5$. Fokin *et al.*[37] developed an alternative correlation for the collision integrals of Lennard-Jones m-6 potentials, to which Fokin and Kalashnikov[36] applied the Brokaw approximation to obtain the viscosity of steam using the Stockmayer potential. We fit the values of $\Omega_{SM}^{(2,2)*}$ tabulated by Monchick and Mason[94] to an empirical function that reduces to the Lennard-Jones 12-6 form when the dipole moment is zero, and obtain

$$\Omega_{SM}^{(2,2)^*}=\Omega_{LJ}^{(2,2)^*}\left[1+\frac{\delta^2}{1+a_6\delta^6}\Omega_{\delta}^{(2,2)^*}\right] \tag{8}$$

with

$$\Omega_{\delta}^{(2,2)^*}=a_7(T^*)^{a_8}+a_9e^{a_{10}T^*}+a_{11}e^{a_{12}T^*}. \tag{9}$$

$\Omega_{SM}^{(2,2)*}$ represents the reduced collision integral for the Stockmayer potential including the contribution from the Lennard-Jones collision integral $\Omega_{LJ}^{(2,2)*}$ in the case of $\delta=0$ and a residual reduced collision integral $\Omega_{\delta}^{(2,2)*}$ in terms of δ. Although Monchick and Mason[94] calculated values of the collision integrals for T^* as low as 0.1, the present correlation is limited to a minimum reduced temperature of $T^*=0.3$. With the parameters a_6–a_{12} listed in Table 3(b), Eqs. (8) and (9) reproduce the values of Monchick and Mason[94] for $\Omega_{SM}^{(2,2)*}$ with an average absolute deviation of 0.4%, a maximum deviation of 2.6%, and a standard deviation of 0.6% in the range of $0.3\leqslant T^*\leqslant 100$ and $0\leqslant\delta\leqslant 2.5$. Combining Eqs. (3), (4), (8), and (9) gives a method for the viscosity of a polar gas in terms of three parameters ε_0, σ_0, and δ, which

TABLE 3. (a) Molecular parameters for the representation of the viscosity of methanol and (b) values for the adjusted parameters in the viscosity correlation for methanol.

(a)

Molar mass	Critical temp. and density (Gude, Teja[55])		Stockmayer potential parameters				Reducing parameter, Eq. (17)
M	T_c	ρ_c	ε_0/k	σ_0	δ	μ	σ_c
32.04216 kg kmol^{-1}	512.6 K	273 kg m^{-3}	577.87 K	0.3408 nm	0.4575	1.7 D	0.7193422 nm

(b)

i	a_i (Eqs. (4) and (8))	b_i Eq. (13)	c_i Eq. (14)	d_i Eq. (17)	e_i Eq. (17)
0	1.16145	−19.572881	1.86222085×10^{-3}	−1.181909	
1	−0.14874	219.73999	9.990338	0.5031030	4.018368
2	0.52487	−1015.3226		−0.6268461	−4.239180
3	−0.77320	2471.0125		0.5169312	2.245110
4	2.16178	−3375.1717		−0.2351349	−0.5750698
5	−2.43787	2491.6597		5.3980235×10^{-2}	2.3021026×10^{-2}
6	$(0.95976\pm0.027)\times10^{-3}$	−787.26086		-4.9069617×10^{-3}	2.5696775×10^{-2}
7	0.10225±0.0058	14.085455			-6.8372749×10^{-3}
8	−0.97346±0.027	−0.34664158			7.2707189×10^{-4}
9	0.10657±0.0064				-2.9255711×10^{-5}
10	−0.34528±0.016				
11	−0.44557±0.049				
12	−2.58055±0.092				

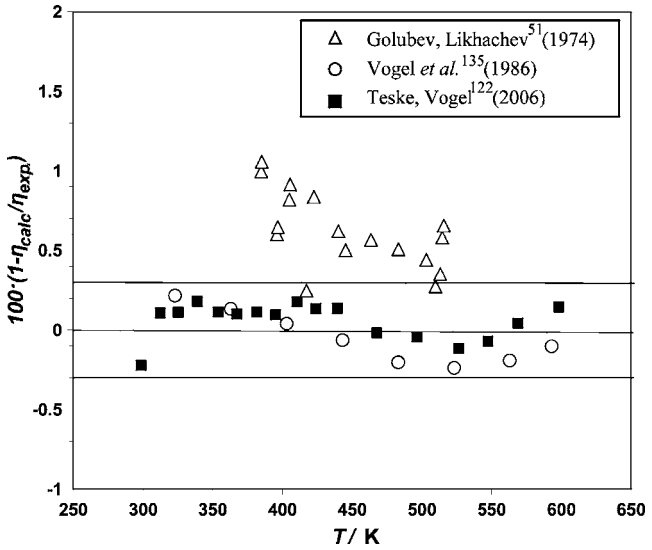

FIG. 4. Comparison of the viscosity data for methanol with values calculated from the present zero-density correlation, Eqs. (3) and (8).

may be determined from experimental viscosity data in the zero-density limit. However, these three parameters are related via the following expression:[94]

$$\sigma_0^3 = 3.6220\mu^2/(\delta\varepsilon_0/k), \tag{10}$$

where σ_0 is in nanometers, μ is in Debyes, ε_0/k is in Kelvins, and δ is the variable when the collision integrals are averaged over all relative orientations. Therefore it is only necessary to determine two parameters from fitting experimental viscosity data, since the third can be obtained from Eq. (10) and the dipole moment μ.

There are several data sets[26,49,51,90,101,111,117,122,125,135] available for methanol gas at low densities, and two sets[122,135] provide viscosity data in the limit of zero density. Vogel *et al.*[135] obtained viscosity data for methanol in the very low-density vapor phase and derived zero-density viscosities between 310 and 615 K. Teske and Vogel[122] remeasured the viscosity of methanol vapor in this all-quartz oscillating disk viscometer of high precision along ten isochores at densities from 0.004 to 0.049 mol L^{-1} over the temperature range 298–598 K, and they also derived the viscosity in the limit of zero density. Teske and Vogel[122] also examined the results of Golubev and Likhachev[51] and derived zero-density viscosities from the measurements of these authors. For primary data we selected the zero-density data of Vogel *et al.*[135] and Teske and Vogel,[122] and fitted the zero-density viscosity using Eq. (10) with 1.7 D for the gas phase dipole moment of methanol.[97] This led to the following values of the three parameters ε_0/k, σ_0, and δ:

$$\varepsilon_0/k = 577.87 \text{ K}, \quad \sigma_0 = 0.3408 \text{ nm}, \quad \delta = 0.4575, \tag{11}$$

also given in Table 3(a). The experimental uncertainty of the data of Vogel *et al.*[135] was reported as 0.3%, while Teske and Vogel[122] quoted 0.2–0.3%, and that of the results of Golubev and Likhachev[51] is estimated at 1%. Figure 4 shows the deviations between the calculated values of gas viscosity and experimental values in the limit of zero density. The correlation represents the primary data to within their experimental uncertainty of 0.3% at the 95% confidence level. At the highest temperatures, decomposition of the samples may occur. Bruno and Straty[19] reported significant decomposition of methanol at temperatures above 473 K. Teske and Vogel[122] paid particular attention to possible decomposition and observed such effects at temperatures consistent with those reported by Bruno and coworkers,[19,20] but did not report data that may have been affected by decomposition.

5.2. Density Dependence in the Gas Phase

Analogous to the virial expansion of the compressibility factor Z, the reduced viscosity $\bar{\eta}_g$ of a gas at low density may be written as a truncated expansion in terms of density up to the quadratic term

$$\bar{\eta}_g = \eta_g/\eta^0 = 1 + B_\eta\rho + C_\eta\rho^2, \tag{12}$$

where η° is the viscosity in the limit of zero density, as given in Eq. (3), and B_η and C_η are the second and third viscosity virial coefficients. In order to obtain an accurate representation of the behavior of the viscosity in the vapor phase, it is important to consider the temperature dependence of the linear density term.[136] Rainwater and Friend[41,108,109] developed a theory for the temperature dependence of B_η for a Lennard-Jones (12-6) potential, whose theory was later improved to fit molecular substances by Bich and Vogel.[10] In order to better represent the behavior at low reduced temperatures, Laesecke developed a structurally optimized correlation for B_η^* as a component of the reference correlation for the viscosity of propane by Vogel *et al.*[136]

$$B_\eta^* = B_\eta(T)/N_A\sigma_0^3 = \sum_{i=0}^{6} b_i/T^{*0.25i} + b_7/T^{*2.5} + b_8/T^{*5.5}. \tag{13}$$

Here B_η is in units of the volume and σ_0 and ε_0 are the Lennard-Jones (12-6) potential parameters. Eq. (13) is also valid over the reduced temperature range $0.3 \leqslant T^* \leqslant 100$. The coefficients b_i given in Vogel *et al.*[136] are reproduced in Table 3(b) for convenience.

In the absence of a theory for the third viscosity virial coefficient C_η^* an empirical correlation was developed for its temperature dependence

$$C_\eta^* = C_\eta/(N_A\sigma_0^3)^2 = c_0 T^{*3} e^{c_1/\sqrt{T^*}}. \tag{14}$$

The coefficients for Eq. (14) were determined by fitting experimental data for C_η reported by Hurly *et al.*[65] and by Wilhelm and Vogel[141] using published values of the Lennard-Jones scaling parameters for argon, krypton, and nitrogen,[10] methane,[137] sulfur hexafluoride,[120] and propane.[136] We determined the Lennard-Jones parameters for carbon tetrafluoride and hexafluoroethane by fitting the zero-density viscosity data of Hurly *et al.*[63] The behavior of the correlation is illustrated in Fig. 5. We then adapted the equation for methanol, fitting the vapor-phase viscosity data of Golubev and

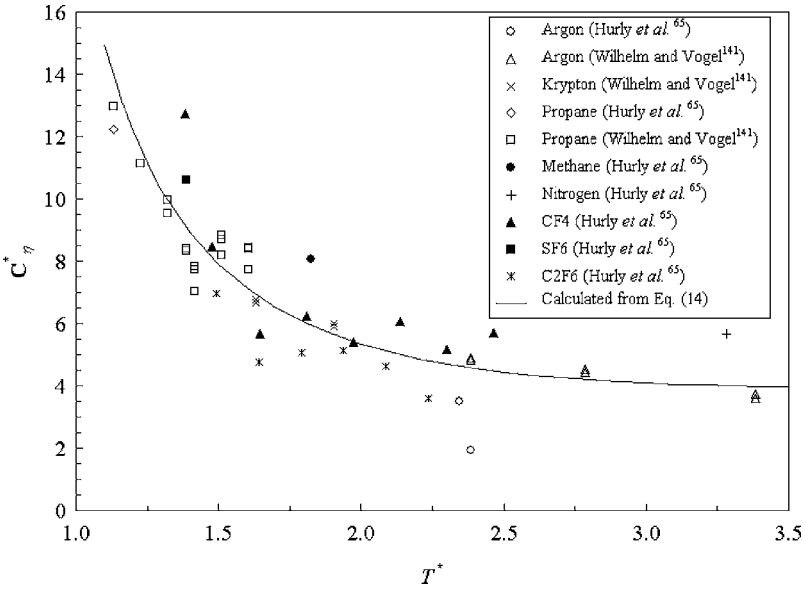

FIG. 5. Third viscosity virial coefficient versus reduced temperature T^*.

Petrov,[47] Vogel *et al.*,[135] and Teske and Vogel[122] and obtained the coefficients in Table 3(b). The equation was scaled so that one set of potential parameters ε_0/k, σ_0 can be used in Eqs. (3), (13), and (14), the resulting coefficients are given in Table 3(b).

Since theory for the second and third viscosity virial coefficients of the polar Stockmayer potential is unavailable, B^*_η and C^*_η for the strongly polar methanol molecule have to be approximated from the nonpolar Lennard-Jones potential. For potential parameters, the values for ε_0/k and σ_0 found from fitting the zero-density data to the Stockmayer potential, Eq. (11), were used. The final representation of the vapor-phase viscosity of methanol in Eq. (12) then is the result of first applying the Stockmayer potential to obtain the zero-density viscosity η° from Eq. (3) with the scaling parameters ε_0/k, σ_0, and δ, followed by the use of the viscosity virial coefficient expressions given in Eqs. (13) and (14).

5.3. High-density Region

Equations (3), (13), and (14) are applicable only in the vapor phase. For dense fluids, we apply the theoretical model of Enskog for the reduced viscosity $\bar{\eta}_E$ of hard spheres[23,33,34]

$$\bar{\eta}_E = \eta_L/\eta_{HS} = 1/g(\sigma_{HS}) + 0.8b\rho + 0.761g(\sigma_{HS})(b\rho)^2, \tag{15}$$

where η_L is the viscosity in the liquid phase and η_{HS} is the viscosity of hard spheres in the limit of zero density. Since the methanol molecule is not really a hard sphere, we set $\eta_{HS}=\eta^\circ$, where η° is the zero-density viscosity from Eq. (3). The radial distribution function for hard spheres at contact, $g(\sigma_{HS})$, was given by Carnahan and Starling,[21]

$$g(\sigma_{HS}) = (1-0.5\xi)/(1-\xi)^3, \tag{16}$$

with the packing fraction $\xi=b\rho/4$, the number or particle density ρ, and the close-packed volume $b=2\pi N_A\sigma^3_{HS}/3$. The temperature and density dependence of σ_{HS} is fitted as follows:

$$\sigma_{HS}/\sigma_c = \sum_{i=0}^{6} d_i/T_r^i + \sum_{j=1}^{9} e_j\rho_r^j \tag{17}$$

where $\rho_r=\rho/\rho_c$ is the reduced density and $T_r=T/T_c$ the reduced temperature. The values of the critical density $\rho_c=273$ kg m^{-3} and critical temperature $T_c=512.6$ K are those of Gude and Teja.[55] We also define the parameter $\sigma_c=(6M/\pi\rho_cN_A)^{1/3}=0.7193422$ nm. Equation (17) combines a dependence on inverse reduced temperature with a dependence on density, which decreases as the temperature increases. The parameters d_i and e_i are given in Table 3(b) as obtained from fitting experimental liquid-phase viscosity data for the primary data, indicated in bold in Table 2. We caution that these parameters do not have physical meaning but are used to correlate the experimental data.

5.4. The Entire Viscosity Surface

In order to represent the entire viscosity surface from the dilute gas to the liquid region, we combine the dilute-gas expression in Eq. (12) with the dense-fluid correlation given in Eq. (15) using a transition function f

$$\eta = \eta^\circ[f\bar{\eta}_g + (1-f)\bar{\eta}_E], \tag{18}$$

where η is the viscosity at any temperature and density over the entire fluid region. The function $f=1/\{1+\exp[5(\rho_r-1)]\}$ is an empirical transition function from the low density to the high density region that reflects the gradual change of molecular interaction mechanisms.

We have omitted a term specific to the critical region. The critical enhancement of the viscosity is observed in only a very small region around the critical point,[40,116,136] and at this time, sufficiently accurate experimental data for methanol are not available in this limited region to support the development of a critical-enhancement term. We note, however,

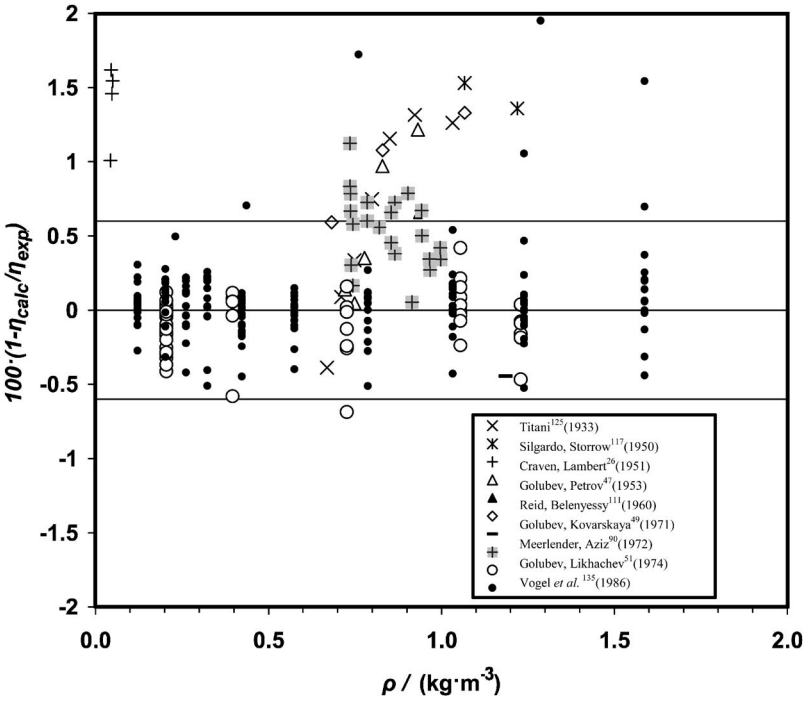

FIG. 6. Percent deviations of the gas-phase viscosity data as a function of density, at very low densities (less than 2 kg m^{-3}) for methanol with values calculated from the present method, Eq. (18).

that according to scaling-law theory the viscosity of a pure fluid at the gas-liquid critical point is infinite.

6. Results and Discussion

Table 2 presents percent deviations of literature data sets with more than two data points from the values calculated with Eq. (18). The following definitions are used:

$$\mathrm{AAD} = \sum_{i=1}^{n} 100|1 - \eta_{i,\mathrm{calc}}/\eta_{i,\mathrm{expt}}|/n, \tag{19}$$

$$\mathrm{bias} = \bar{\eta} = \sum_{i=1}^{n} 100(1 - \eta_{i,\mathrm{calc}}/\eta_{i,\mathrm{expt}})/n, \tag{20}$$

$$\mathrm{RMS} = \sqrt{\sum_{i=1}^{n} [100(1 - \eta_{i,\mathrm{calc}}/\eta_{i,\mathrm{expt}}) - \bar{\eta}]^2/n}, \tag{21}$$

and the maximum percent deviation (Max. Dev.) is listed as well. In Figs. 6–8 we compare selected experimental viscosity data in the vapor and liquid phases with the correlation, Eq. (18). Figure 6 gives the deviations from the experimental data for the vapor-phase viscosity of methanol. Figures 7(a) and 7(b) show deviations of the correlation from the primary data as a function of density, while Fig. 8 presents the deviations as a function of pressure. In general, Figs. 6–8 demonstrate that the present correlation provides a good representation of the viscosity of methanol from very low density to very high pressure.

Figure 6 gives comparisons of viscosity data of methanol vapor at very low densities (less than 2 kg m^{-3}). Primary data used in the correlation are the results by Vogel *et al.*[135] as well as Teske and Vogel.[122] The new correlation reproduces the data of Vogel and collaborators to within 0.6% at the 95% confidence level. Substantial data sets were contributed by Golubev and Petrov,[47] Golubev and Kovarskaya,[49] as well as Golubev and Likhachev.[51] The data of Golubev and Likhachev[51] are also represented well; their estimated uncertainty is 1%. With the exception of the data of Pal and Barua[101] (not shown due to large deviations of 3–8%) the low-density experimental data in the vapor phase are represented by the correlation consistent with their estimated uncertainties.

Figure 7(a) displays the deviations of selected primary data at densities from 100 to 1000 kg m^{-3}. In the mid-density region, the experimental results of Golubev and Petrov[47] exhibit large scatter below 600 kg m^{-3}, but for liquid phase points below 510 K the deviations are within about 3%. There are higher deviations along the isotherms 523.15 and 543.15 K; although these isotherms are close to the critical isotherm, it seems that the large deviations are not due to the lack of a critical enhancement term in the present correlation. Rather, the fluid flow in the capillary viscometer may have been affected at these pressures and temperatures by compressibility effects, which were not considered in the data analysis because an understanding was developed only later by van den Berg *et al.*[131] The results of Blokker[12] also scatter considerably bracketing the deviations of the results of Golubev and Petrov.[47] The atmospheric pressure data of Mitsukuri and Tonomura,[92] Hammond *et al.*,[56] Lee *et al.*,[81] and Soliman and Marschall,[118] show deviations within 2%. At pressures up to 30 MPa, the data of Matsuo and Makita[88] and Assael and Polimatidou[7] also deviate within about 2%. The data of Weber[138] extend to higher pressures of 50 MPa and deviate within 3%.

Figure 7(b) shows deviations between several data sets at

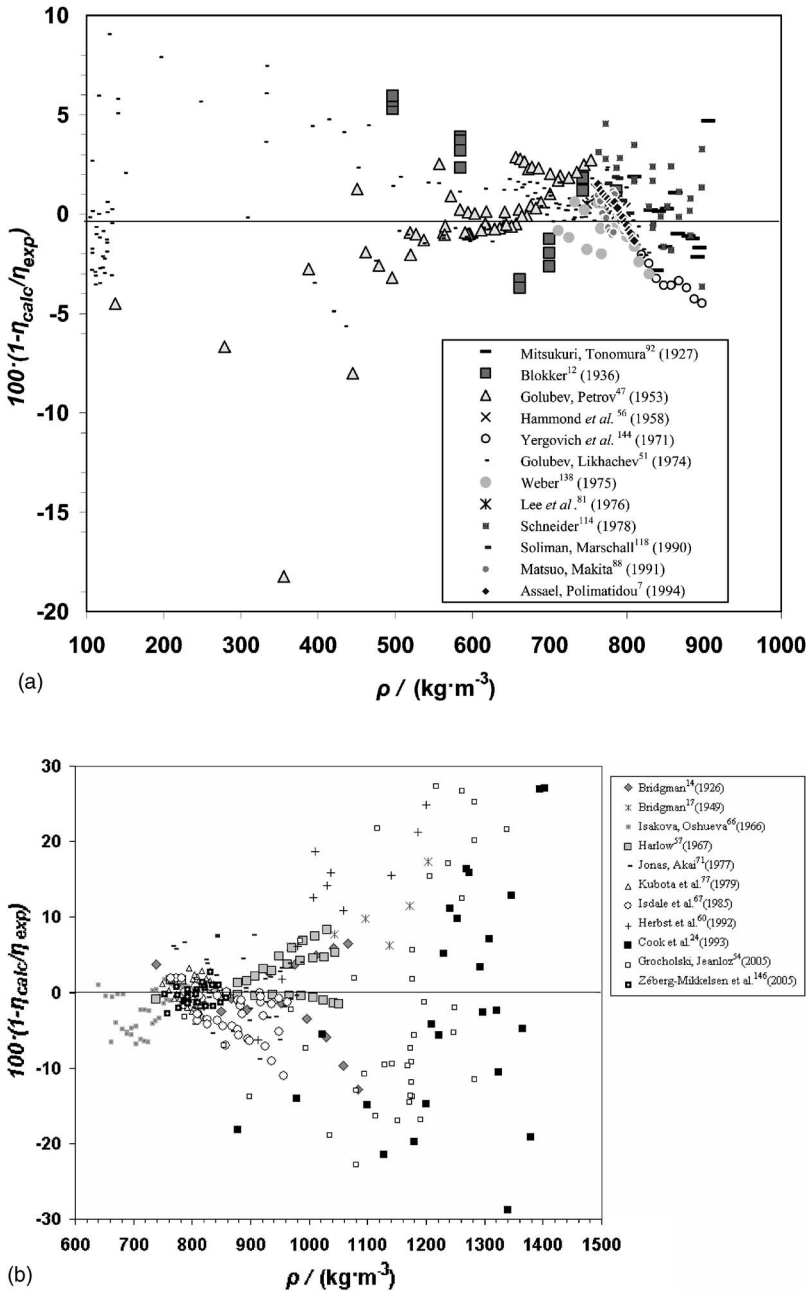

FIG. 7. (a) Percent deviations as a function of density (100–1000 kg m^{-3}) of selected viscosity data for methanol from values calculated from the present method, Eq. (18); and (b) percent deviations as a function of density (600–1500 kg m^{-3}) of selected viscosity data for methanol from values calculated from the present method, Eq. (18).

elevated pressures and the correlation in the density range from 600 to 1500 kg m^{-3}. The deviations of the early high-pressure data sets of Bridgman[14,17] deviate in opposite direction to maxima of 17% and −13%. The quoted uncertainty of the data by Isakova and Oshueva[66] is 1% but their average absolute deviation from the correlation is 2.4%. The data of Harlow[57] were measured in a falling-cylinder viscometer with a quoted uncertainty of 1.4%. They are represented to within 2% at pressures up to 500 MPa and to within 4% to their maximum pressure of 935 MPa. The data of Jonas and Akai[71] were measured with a rolling-sphere viscometer on deuterated methanol in a wide range of temperatures from 223 to 323 K with pressures up to 500 MPa. While their quoted experimental uncertainty is 3%, their deviations from the correlation scatter unsystematically up to a maximum of −8.9%. The results of Kubota *et al.*[77] were obtained in a falling-cylinder viscometer and are represented within their quoted uncertainty of 2%. The data of Isdale *et al.*[67] with a quoted uncertainty of 2% cover a pressure range similar to those of Harlow[57] but show larger deviations; up to −5% at pressures below 100 MPa, and up to −10% at 500 MPa, with the largest deviations at the lowest temperature, 298 K. The data of Zéberg-Mikkelsen *et al.*[146] obtained with a falling-body method with quoted uncertainty of 2%, cover pressures up to 100 MPa, and have an average absolute deviation of 1% with a maximum deviation of −2.8%. We became aware of this set after the development of the correlation, and it was not used in the determination of the coefficients.

As mentioned in Sec. 4, methanol is among those fluids whose viscosity has been investigated to extremely high

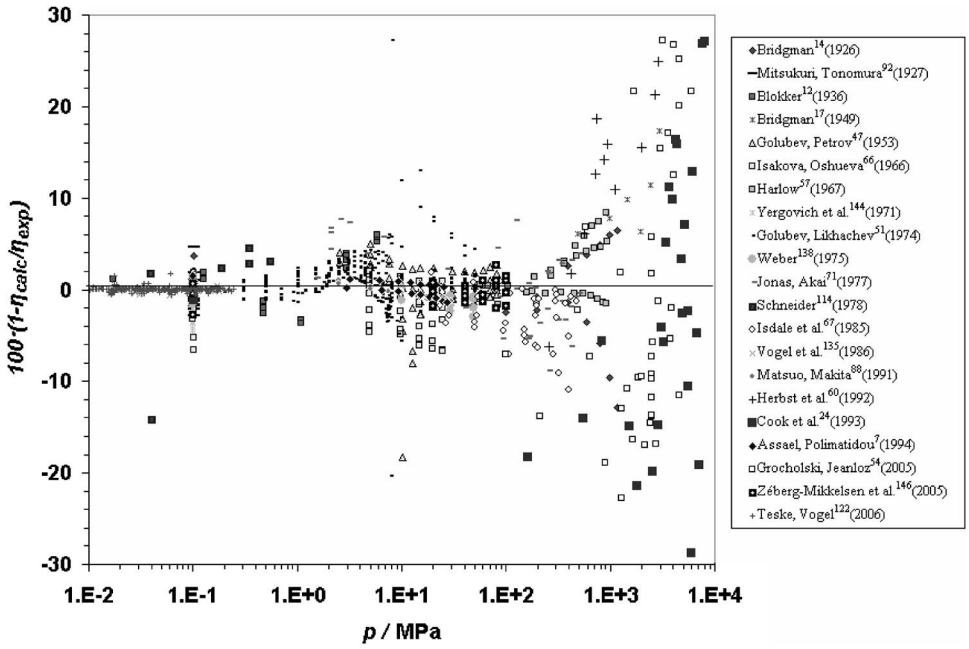

FIG. 8. Percent deviations as a function of pressure of selected viscosity data for methanol from values calculated from the present method, Eq. (18).

TABLE 4. Summary of the correlation

Equations are numbered as they appear in the text. Parameters are listed in Tables 3(a) and (b).

The viscosity of methanol developed in this work is

$$\eta = \eta^\circ [f \bar{\eta}_g + (1-f)\bar{\eta}_E], \tag{18}$$

with the transition function $f = 1/\{1+\exp[5(\rho_r - 1)]\}$, where $\rho_r = \rho/\rho_c$, and the truncated virial expansion for the viscosity in the vapor region

$$\bar{\eta}_g = 1 + B_\eta(T)\rho + C_\eta(T)\rho^2$$

Viscosity in the zero-density limit

$$\eta^\circ = 5\sqrt{mkT/\pi}/(16\sigma_0^2\Omega^{(2,2)*}) \tag{3}$$

or alternatively in SI units (Pa s, K, m) $\eta^\circ = 2.66957\cdot 10^{-26}\sqrt{MT}/(\sigma_0^2\Omega^{(2,2)*})$.

The following parameterization of the reduced collision integral of the Stockmayer potential is developed in this work:

$$\Omega^{(2,2)*}_{SM} = \Omega^{(2,2)*}_{LJ}\left[1 + \frac{\delta^2}{1+a_6\delta^6}\Omega^{(2,2)*}_{\delta}\right] \tag{8}$$

The correlation of the reduced collision integral of the Lennard-Jones potential was developed by Neufeld *et al.*[98]

$$\Omega^{(2,2)*}_{LJ} = a_0(T^*)^{a_1} + a_2 e^{a_3 T^*} + a_4 e^{a_5 T^*} \tag{4}$$

with $T^* = kT/\varepsilon_0$.

This was adopted in this work for the residual collision integral:

$$\Omega^{(2,2)*}_{\delta} = a_7(T^*)^{a_8} + a_9 e^{a_{10}T^*} + a_{11}e^{a_{12}T^*} \tag{9}$$

Second viscosity virial coefficient:

$$B^*_\eta = B_\eta(T)/N_A\sigma_0^3 = \Sigma_{i=0}^{6} b_i/T^{*0.251i} + b_7/T^{*2.5} + b_8/T^{*5.5} \tag{13}$$

Third viscosity virial coefficient:

$$C^*_\eta = C_\eta/(N_A\sigma_0^3)^2 = c_0 T^{*3} e^{c_1/\sqrt{T^*}} \tag{14}$$

The reduced viscosity at high density according to the Enskog theory is:

$$\bar{\eta}_E = \eta_L/\eta_{HS} = 1/g(\sigma_{HS}) + 0.8b\rho + 0.761 g(\sigma_{HS})(b\rho)^2, \tag{15}$$

$$g(\sigma_{HS}) = (1-0.5\xi)/(1-\xi)^3, \tag{16}$$

with $\xi = b\rho/4$ and $b = 2\pi N_A\sigma_{HS}^3/3$. σ_{HS} is developed in this work,

$$\sigma_{HS}/\sigma_c = \sum_{i=0}^{6} d_i/T_r^i + \sum_{j=1}^{9} e_j\rho_r^j \tag{17}$$

with the fitted parameters d_i, e_i, and σ_c as given in Tables 3(a) and (b).

pressures. As seen in Figs. 2(a) and 8, the maximum pressure of 8.35 GPa was attained in the viscosity measurements of Cook *et al.*[24] with an ingenious rolling sphere in a diamond anvil cell mounted on a centrifuge. The correlation does not represent the data at such high pressures to within their estimated uncertainty of 2.8–12%; however no systematic trends are apparent and the correlation can be used in a qualitative manner to represent the viscosity behavior at these extreme conditions. Other high-pressure data whose deviations are shown in Fig. 7(b) are the light-scattering data by Herbst *et al.*,[60] from the same laboratory as those of Cook *et al.*,[24] as well as the measurements of Grocholski and Jeanloz[54] and by Zéberg-Mikkelsen *et al.*[146] The deviations as a function of density in Fig. 7(b) and as a function of pressure in Fig. 8 suggest that the new correlation represents the data at extreme pressures consistently albeit not within their quoted experimental uncertainty. However, the data sets of Cook *et al.*[24] and Grocholski and Jeanloz[54] appear to lack consistency in the viscosity–density diagram, Fig. 2(b). At this time, there is not enough information for a final evaluation of the uncertainties of these experimental results.

Some data points of Cook *et al.*[24] and Grocholski and Jeanloz[54] are in the metastable, supercompressed region above the melting pressure [cf. Fig. 2(a)]. The deviations of their viscosities from the new correlation suggest that the correlation can be used in this region to a certain extent. However, the functional form of the correlation is not suitable to predict the increase of the viscosity at lower temperatures and/or higher pressures.

7. Tabulations and Overall Uncertainty Assessment

To facilitate its implementation, Table 4 presents a summary of the new viscosity correlation for methanol. Tables 5 and 6 list calculated viscosity and density data of methanol along the saturation boundary and in the single-phase region for pressures up to 800 MPa. Equation (18) was used to compute the values of the viscosity, while the densities are from the equation of state of de Reuck and Craven.[28] The tables provide reference values and may also be used to validate computer codes. Figure 9 summarizes the estimated uncertainties of the present correlation. Uncertainties in the light gray regions are based on comparisons with experimental data, while those in the dark gray regions are estimated. Figure 10 shows the three-dimensional viscosity surface as a function of temperature and density calculated from the present correlation, Eq. (18). It should be noted that the viscosity is shown on a logarithmic scale covering more than 4 orders of magnitude.

It is also noted that the correlation yields negative viscosity values in a small part of the two-phase region near the saturated vapor locus at low temperatures. This behavior is physically not meaningful and arises due to the negative second viscosity virial coefficient B_η not being sufficiently balanced in that region by the third viscosity virial coefficient C_η. Some applications of corresponding states may enter this region during iterations and it may be a concern for some users of the correlation. This artifact will be avoided effectively once the temperature dependence of the third viscosity virial coefficient $C_\eta(T)$ is elucidated by progress in extending the Rainwater–Friend theory.

8. Conclusions and Recommendations for Further Study

We present a new reference-quality correlation for the viscosity of methanol that combines the kinetic theory for the dilute gas, Rainwater–Friend theory for the initial density dependence, the third viscosity virial coefficient for the quadratic density dependence in the vapor phase, and Enskog hard-sphere theory for the high-density fluid region. The viscosity behavior is described over the entire fluid domain including gas, liquid, and supercritical states in a unified way. The model contains empirical parameters but is based in part on kinetic theory. The correlation in this work is specific for methanol and contains parameters determined by regression of the experimental data; however, the approach is general and can be applied to other polar and nonpolar fluids as well. The resulting correlation is applicable for temperatures from the triple point to 630 K at pressures up to 8 GPa. The uncertainty of the resulting correlation (with a coverage factor of 2) varies from 0.6% in the dilute-gas phase between room temperature and 630 K, to less than 2% for the liquid phase at pressures up to 30 MPa at temperatures between 273 and 343 K, 3% for pressures from 30 to 100 MPa, 5% for the liquid from 100 to 500 MPa, and 10% between 500 MPa and 4 GPa. At very high pressures, from 4 to 8 GPa, the correlation has an estimated uncertainty of 30% and can be used qualitatively.

There is a need for additional measurements to resolve discrepancies in density measurements at very high pressures as a prerequisite for better correlations of the viscosity, and to the development of improved equations of state for methanol. Particularly desirable are further viscosity measurements in three regions. Apparent from Fig. 2(b) is the sparsity of the available viscosity data for methanol in the density range from 100 to 500 kg m^{-3}. The corresponding pressure range is indicated by the isochors in Fig. 9. While it may appear small, measurements in this range should be carried out in small pressure increments because of the steep slopes of the density and viscosity surfaces. A second region of priority for further viscosity measurements is the temperature range from the triple point (175.91 K) to approximately 300 K with pressures from the vapor pressure curve to the melting pressure curve and possibly beyond. Such measurements are needed to resolve the temperature dependence of the viscosity surface that is delineated in Fig. 2(b) by the data sets of Mitsukuri and Tonomura[92] as well as Cook *et al.*[24] and Grocholski and Jeanloz.[54] Finally, further viscosity measurements would be useful in the temperature range from

TABLE 5. Viscosity and density of methanol along the saturation curve

		Saturated vapor		Saturated liquid	
T (K)	p (Mpa)	ρ/(kg m^{-3})	η/(mPa s)	ρ/(kg m^{-3})	η/(mPa s)
175.63	0.000000186	0.00000409	0.005822	904.56	12.80
180	0.000000376	0.00000806	0.005954	900.27	10.44
185	0.000000802	0.00001671	0.006106	895.30	8.274
190	0.000001638	0.00003323	0.006258	890.29	6.641
195	0.000003217	0.00006362	0.006410	885.28	5.424
200	0.000006096	0.00011754	0.006563	880.28	4.506
205	0.000011169	0.00021017	0.006716	875.30	3.802
210	0.000019841	0.00036456	0.006869	870.35	3.251
215	0.000034246	0.00061485	0.007023	865.41	2.811
220	0.00005755	0.0010102	0.007178	860.50	2.454
225	0.00009433	0.0016199	0.007333	855.62	2.158
230	0.00015106	0.0025394	0.007488	850.75	1.911
235	0.00023672	0.0038976	0.007643	845.91	1.702
240	0.00036348	0.0058649	0.007799	841.09	1.523
245	0.00054757	0.0086634	0.007956	836.29	1.370
250	0.0008103	0.012577	0.008112	831.52	1.236
255	0.0011791	0.017964	0.008269	826.76	1.120
260	0.0016889	0.025270	0.008426	822.03	1.019
265	0.0023834	0.035039	0.008583	817.31	0.9294
270	0.0033166	0.047933	0.008740	812.60	0.8505
275	0.0045545	0.064742	0.008897	807.91	0.7806
280	0.0061769	0.086401	0.009054	803.23	0.7185
285	0.0082787	0.11401	0.009211	798.55	0.6631
290	0.010972	0.14884	0.009367	793.87	0.6135
295	0.014390	0.19235	0.009523	789.19	0.5691
300	0.018682	0.24623	0.009678	784.51	0.5291
305	0.024026	0.31237	0.009833	779.81	0.4931
310	0.030621	0.39291	0.009987	775.08	0.4604
315	0.038692	0.49025	0.01014	770.34	0.4308
320	0.048494	0.60706	0.01029	765.56	0.4039
325	0.060310	0.74629	0.01044	760.74	0.3794
330	0.074453	0.91122	0.01059	755.88	0.3569
335	0.09127	1.1054	0.01074	750.97	0.3363
340	0.11114	1.3329	0.01089	746.00	0.3174
345	0.13447	1.5979	0.01103	740.96	0.2999
350	0.16172	1.9053	0.01118	735.84	0.2838
355	0.19337	2.2601	0.01132	730.65	0.2688
360	0.22992	2.6681	0.01146	725.36	0.2550
365	0.27195	3.1354	0.01160	719.97	0.2420
370	0.32004	3.6688	0.01173	714.47	0.2300
375	0.37483	4.2757	0.01187	708.86	0.2187
380	0.43697	4.9644	0.01200	703.11	0.2081
385	0.50717	5.7440	0.01213	697.22	0.1981
390	0.58617	6.6244	0.01226	691.18	0.1887
395	0.67476	7.6170	0.01239	684.98	0.1798
400	0.77374	8.7343	0.01251	678.59	0.1714
405	0.88399	9.9905	0.01264	672.01	0.1635
410	1.0064	11.401	0.01276	665.22	0.1559
415	1.1419	12.985	0.01289	658.20	0.1487
420	1.2914	14.762	0.01301	650.93	0.1418
425	1.4561	16.754	0.01314	643.38	0.1352
430	1.6369	18.987	0.01327	635.53	0.1288
435	1.8349	21.486	0.01341	627.35	0.1227
440	2.0513	24.277	0.01356	618.82	0.1169
445	2.2870	27.385	0.01371	609.88	0.1113
450	2.5433	30.831	0.01388	600.49	0.1058
455	2.8212	34.634	0.01407	590.60	0.1006
460	3.1216	38.821	0.01428	580.14	0.09550
465	3.4456	43.433	0.01451	569.03	0.09056
470	3.7942	48.558	0.01479	557.15	0.08576
475	4.1688	54.371	0.01511	544.35	0.08107
480	4.5713	61.206	0.01550	530.40	0.07646
485	5.0047	69.666	0.01599	514.95	0.07189
490	5.4732	80.371	0.01667	497.41	0.06728
495	5.9794	93.083	0.01758	476.79	0.06253
500	6.5250	109.88	0.01891	451.53	0.05748
505	7.1164	132.87	0.02101	420.32	0.05217
510	7.7496	165.68	0.02440	374.56	0.04570
512	8.0195	202.99	0.02838	341.17	0.04174
512.6	8.1	273	∞	273	∞

TABLE 6. Viscosity and density of methanol as a function of pressure and temperature

	180		200		220	
T (K) p (MPa)	ρ/(kg m^{-3})	η/(mPa s)	ρ/(kg m^{-3})	η/(mPa s)	ρ/(kg m^{-3})	η/(mPa s)
0.01	900.27	10.44	880.29	4.507	860.51	2.454
0.05	900.29	10.45	880.31	4.508	860.54	2.455
0.10	900.32	10.45	880.34	4.510	860.57	2.455
0.15	900.34	10.46	880.37	4.511	860.60	2.456
0.20	900.37	10.46	880.40	4.513	860.63	2.457
0.25	900.39	10.47	880.43	4.515	860.67	2.458
0.30	900.42	10.47	880.45	4.516	860.70	2.459
0.35	900.44	10.47	880.48	4.518	860.73	2.459
0.40	900.47	10.48	880.51	4.519	860.76	2.460
0.45	900.49	10.48	880.54	4.521	860.80	2.461
0.50	900.52	10.49	880.57	4.523	860.83	2.462
0.60	900.57	10.50	880.63	4.526	860.89	2.463
0.80	900.66	10.51	880.74	4.533	861.02	2.467
1.00	900.76	10.53	880.86	4.539	861.15	2.470
1.50	901.01	10.58	881.14	4.556	861.47	2.478
2.00	901.25	10.62	881.43	4.572	861.79	2.486
2.50	901.50	10.67	881.72	4.589	862.11	2.494
3.00	901.74	10.71	882.00	4.605	862.43	2.502
3.50	901.98	10.76	882.28	4.622	862.75	2.510
4.00	902.22	10.80	882.57	4.639	863.07	2.518
5.00	902.71	10.89	883.13	4.672	863.70	2.535
6.00	903.18	10.98	883.69	4.705	864.32	2.551
8.00	904.14	11.17	884.80	4.773	865.56	2.583
10.0	905.08	11.36	885.90	4.840	866.79	2.616
15.0	907.39	11.83	888.59	5.012	869.78	2.698
20.0	909.65	12.33	891.21	5.187	872.69	2.781
25.0	911.86	12.84	893.77	5.365	875.52	2.864
30.0			896.26	5.546	878.27	2.948
35.0			898.70	5.732	880.95	3.034
40.0			901.08	5.921	883.57	3.120
50.0			905.70	6.312	888.63	3.296
60.0			910.14	6.721	893.47	3.476
80.0			918.54	7.597	902.59	3.853
100			926.38	8.560	911.07	4.253
150			944.08	11.44	930.07	5.376
200					946.71	6.721
250					961.59	8.350
300					975.09	10.35
350					987.49	12.82

	240		260		280	
T (K) p (MPa)	ρ/(kg m^{-3})	η/(mPa s)	ρ/(kg m^{-3})	η/(mPa s)	ρ/(kg m^{-3})	η/(mPa s)
0.01	841.10	1.524	822.03	1.019	803.23	0.7185
0.05	841.13	1.524	822.07	1.019	803.27	0.7187
0.10	841.16	1.524	822.11	1.019	803.31	0.7189
0.15	841.20	1.525	822.15	1.020	803.36	0.7191
0.20	841.24	1.525	822.19	1.020	803.40	0.7193
0.25	841.27	1.526	822.23	1.020	803.45	0.7195
0.30	841.31	1.526	822.27	1.021	803.49	0.7198
0.35	841.35	1.527	822.31	1.021	803.54	0.7200
0.40	841.38	1.527	822.35	1.021	803.58	0.7202
0.45	841.42	1.528	822.39	1.022	803.63	0.7204
0.50	841.45	1.528	822.43	1.022	803.67	0.7206
0.60	841.53	1.529	822.51	1.022	803.76	0.7211
0.80	841.67	1.531	822.67	1.024	803.94	0.7219
1.00	841.81	1.533	822.83	1.025	804.12	0.7228
1.50	842.17	1.538	823.23	1.028	804.56	0.7250
2.00	842.53	1.542	823.63	1.031	805.00	0.7272
2.50	842.89	1.547	824.02	1.034	805.44	0.7293

TABLE 6. Viscosity and density of methanol as a function of pressure and temperature—Continued

	240		260		280	
T (K) p (MPa)	ρ/(kg m^{-3})	η/(mPa s)	ρ/(kg m^{-3})	η/(mPa s)	ρ/(kg m^{-3})	η/(mPa s)
3.00	843.24	1.552	824.41	1.037	805.88	0.7315
3.50	843.59	1.557	824.81	1.040	806.32	0.7337
4.00	843.95	1.561	825.20	1.043	806.75	0.7358
5.00	844.65	1.571	825.97	1.050	807.61	0.7401
6.00	845.34	1.580	826.74	1.056	808.46	0.7444
8.00	846.71	1.599	828.26	1.068	810.13	0.7529
10.0	848.07	1.618	829.75	1.080	811.78	0.7614
15.0	851.37	1.665	833.38	1.110	815.76	0.7823
20.0	854.56	1.712	836.88	1.140	819.58	0.8028
25.0	857.65	1.759	840.25	1.170	823.26	0.8232
30.0	860.66	1.806	843.51	1.199	826.80	0.8433
35.0	863.57	1.854	846.68	1.229	830.22	0.8632
40.0	866.42	1.901	849.74	1.258	833.53	0.8830
50.0	871.88	1.997	855.63	1.317	839.86	0.9221
60.0	877.09	2.094	861.22	1.376	845.83	0.9608
80.0	886.86	2.293	871.63	1.494	856.91	1.038
100	895.89	2.498	881.21	1.613	867.04	1.114
150	915.99	3.050	902.36	1.924	889.24	1.307
200	933.45	3.671	920.58	2.258	908.23	1.507
250	948.97	4.380	936.69	2.623	924.93	1.718
300	963.00	5.197	951.19	3.025	939.89	1.944
350	975.84	6.145	964.42	3.472	953.50	2.186
400	987.71	7.252	976.61	3.972	966.00	2.449
500	1009.1	10.09	998.52	5.165	988.41	3.048
600	1028.1	14.11	1017.9	6.693	1008.1	3.767
800			1051.2	11.27	1041.9	5.698

	300		320		340	
T (K) p (MPa)	ρ/(kg m^{-3})	η/(mPa s)	ρ/(kg m^{-3})	η/(mPa s)	ρ/(kg m^{-3})	η/(mPa s)
0.01	0.12955	0.009696	0.12096	0.01035	0.11369	0.01101
0.05	784.54	0.5292	765.56	0.4039	0.57636	0.01097
0.10	784.59	0.5294	765.62	0.4040	1.1872	0.01090
0.15	784.64	0.5296	765.67	0.4042	746.05	0.3175
0.20	784.69	0.5297	765.73	0.4043	746.11	0.3176
0.25	784.74	0.5299	765.79	0.4044	746.17	0.3177
0.30	784.79	0.5301	765.84	0.4046	746.24	0.3178
0.35	784.84	0.5302	765.90	0.4047	746.30	0.3179
0.40	784.89	0.5304	765.96	0.4048	746.37	0.3180
0.45	784.94	0.5305	766.01	0.4050	746.43	0.3181
0.50	784.99	0.5307	766.07	0.4051	746.49	0.3182
0.60	785.09	0.5310	766.18	0.4054	746.62	0.3185
0.80	785.29	0.5317	766.40	0.4059	746.87	0.3189
1.00	785.49	0.5324	766.63	0.4064	747.13	0.3194
1.50	785.98	0.5340	767.18	0.4078	747.75	0.3205
2.00	786.47	0.5357	767.73	0.4091	748.38	0.3216
2.50	786.96	0.5373	768.28	0.4104	749.00	0.3227
3.00	787.45	0.5389	768.82	0.4117	749.61	0.3238
3.50	787.93	0.5405	769.36	0.4130	750.22	0.3249
4.00	788.41	0.5422	769.90	0.4143	750.82	0.3260
5.00	789.37	0.5454	770.96	0.4168	752.02	0.3281
6.00	790.31	0.5486	772.01	0.4194	753.19	0.3302
8.00	792.16	0.5550	774.07	0.4244	755.50	0.3345
10.0	793.98	0.5613	776.08	0.4294	757.74	0.3386
15.0	798.36	0.5768	780.90	0.4416	763.09	0.3487
20.0	802.53	0.5919	785.48	0.4534	768.14	0.3584
25.0	806.53	0.6068	789.85	0.4650	772.91	0.3679
30.0	810.37	0.6214	794.02	0.4763	777.46	0.3770
35.0	814.07	0.6359	798.02	0.4873	781.80	0.3860
40.0	817.64	0.6501	801.86	0.4982	785.96	0.3947

TABLE 6. Viscosity and density of methanol as a function of pressure and temperature—Continued

	300		320		340	
T (K) p (MPa)	ρ/(kg m^{-3})	η/(mPa s)	ρ/(kg m^{-3})	η/(mPa s)	ρ/(kg m^{-3})	η/(mPa s)
50.0	824.43	0.6781	809.15	0.5194	793.81	0.4117
60.0	830.81	0.7055	815.98	0.5401	801.11	0.4281
80.0	842.59	0.7592	828.49	0.5801	814.42	0.4595
100	853.28	0.8119	839.78	0.6188	826.35	0.4894
150	876.57	0.9418	864.18	0.7121	851.93	0.5605
200	896.33	1.072	884.74	0.8036	873.32	0.6284
250	913.62	1.206	902.64	0.8953	891.85	0.6953
300	929.06	1.346	918.57	0.9889	908.28	0.7624
350	943.05	1.492	932.96	1.085	923.09	0.8304
400	955.88	1.648	946.13	1.186	936.61	0.9002
500	978.80	1.989	969.59	1.401	960.65	1.047
600	998.93	2.382	990.14	1.640	981.64	1.206
800	1033.3	3.364	1025.1	2.211	1017.3	1.572

	360		380		400	
T (K) p (MPa)	ρ/(kg m^{-3})	η/(mPa s)	ρ/(kg m^{-3})	η/(mPa s)	ρ/(kg m^{-3})	η/(mPa s)
0.01	0.10728	0.01168	0.10158	0.01235	0.096463	0.01302
0.05	0.54125	0.01164	0.51125	0.01232	0.48474	0.01300
0.10	1.0966	0.01159	1.0314	0.01228	0.97575	0.01297
0.15	1.6720	0.01154	1.5616	0.01224	1.4734	0.01294
0.20	2.2797	0.01149	2.1038	0.01220	1.9784	0.01290
0.25	725.39	0.2550	2.6606	0.01216	2.4911	0.01287
0.30	725.46	0.2551	3.2359	0.01212	3.0126	0.01284
0.35	725.54	0.2552	3.8354	0.01208	3.5438	0.01281
0.40	725.61	0.2553	4.4678	0.01203	4.0859	0.01277
0.45	725.68	0.2554	703.13	0.2081	4.6405	0.01274
0.50	725.76	0.2555	703.22	0.2082	5.2095	0.01271
0.60	725.90	0.2557	703.39	0.2084	6.4011	0.01264
0.80	726.20	0.2561	703.74	0.2087	678.65	0.1715
1.00	726.49	0.2565	704.08	0.2091	679.07	0.1718
1.50	727.21	0.2575	704.94	0.2100	680.12	0.1727
2.00	727.93	0.2585	705.78	0.2109	681.15	0.1736
2.50	728.64	0.2594	706.61	0.2118	682.16	0.1745
3.00	729.34	0.2604	707.44	0.2127	683.16	0.1754
3.50	730.04	0.2614	708.25	0.2136	684.14	0.1762
4.00	730.73	0.2623	709.06	0.2145	685.11	0.1771
5.00	732.09	0.2642	710.64	0.2162	687.02	0.1788
6.00	733.43	0.2661	712.20	0.2180	688.87	0.1804
8.00	736.04	0.2698	715.21	0.2213	692.44	0.1836
10.0	738.56	0.2734	718.11	0.2246	695.85	0.1867
15.0	744.56	0.2821	724.93	0.2325	703.76	0.1941
20.0	750.17	0.2905	731.24	0.2400	710.97	0.2011
25.0	755.44	0.2986	737.12	0.2472	717.62	0.2077
30.0	760.43	0.3064	742.64	0.2541	723.80	0.2140
35.0	765.17	0.3139	747.85	0.2607	729.59	0.2200
40.0	769.69	0.3213	752.79	0.2672	735.04	0.2258
50.0	778.16	0.3355	762.00	0.2795	745.12	0.2369
60.0	786.01	0.3491	770.46	0.2912	754.30	0.2473
80.0	800.19	0.3748	785.62	0.3132	770.58	0.2667
100	812.81	0.3992	799.01	0.3337	784.82	0.2846
150	839.65	0.4558	827.21	0.3808	814.50	0.3251
200	861.91	0.5089	850.40	0.4240	838.68	0.3616
250	881.10	0.5603	870.28	0.4652	859.29	0.3958
300	898.06	0.6110	887.79	0.5053	877.38	0.4287
350	913.31	0.6618	903.49	0.5450	893.55	0.4609
400	927.20	0.7132	917.77	0.5847	908.23	0.4928
500	951.83	0.8196	943.04	0.6658	934.16	0.5571
600	973.30	0.9326	965.01	0.7505	956.66	0.6234
800	1009.7	1.186	1002.1	0.9363	994.59	0.7662

TABLE 6. Viscosity and density of methanol as a function of pressure and temperature—Continued

	420		440		460	
T (K) p (MPa)	ρ/(kg m^{-3})	η/(mPa s)	ρ/(kg m^{-3})	η/(mPa s)	ρ/(kg m^{-3})	η/(mPa s)
0.01	0.091845	0.01370	0.087653	0.01438	0.083830	0.01506
0.05	0.46102	0.01368	0.43962	0.01436	0.42019	0.01505
0.10	0.92664	0.01365	0.88270	0.01434	0.84304	0.01503
0.15	1.3971	0.01363	1.3294	0.01432	1.2686	0.01501
0.20	1.8725	0.01360	1.7797	0.01430	1.6970	0.01499
0.25	2.3533	0.01358	2.2339	0.01428	2.1282	0.01497
0.30	2.8396	0.01355	2.6920	0.01426	2.5624	0.01496
0.35	3.3319	0.01352	3.1543	0.01423	2.9997	0.01494
0.40	3.8304	0.01350	3.6209	0.01421	3.4400	0.01492
0.45	4.3357	0.01347	4.0920	0.01419	3.8836	0.01491
0.50	4.8481	0.01345	4.5677	0.01417	4.3305	0.01489
0.60	5.8968	0.01339	5.5339	0.01413	5.2347	0.01486
0.80	8.1100	0.01329	7.5326	0.01405	7.0879	0.01479
1.00	10.537	0.01318	9.6358	0.01397	9.0076	0.01473
1.50	651.49	0.1421	15.557	0.01377	14.171	0.01458
2.00	652.81	0.1430	23.289	0.01357	20.061	0.01444
2.50	654.11	0.1439	620.44	0.1178	27.120	0.01433
3.00	655.39	0.1448	622.20	0.1187	36.174	0.01427
3.50	656.63	0.1457	623.92	0.1197	582.19	0.09634
4.00	657.86	0.1466	625.58	0.1206	584.79	0.09743
5.00	660.25	0.1482	628.79	0.1224	589.65	0.09950
6.00	662.55	0.1499	631.84	0.1241	594.15	0.1015
8.00	666.94	0.1531	637.56	0.1275	602.26	0.1051
10.0	671.08	0.1562	642.83	0.1306	609.47	0.1085
15.0	680.53	0.1634	654.52	0.1379	624.75	0.1161
20.0	688.95	0.1700	664.66	0.1445	637.39	0.1229
25.0	696.60	0.1763	673.65	0.1506	648.28	0.1290
30.0	703.62	0.1822	681.78	0.1564	657.90	0.1347
35.0	710.14	0.1879	689.22	0.1618	666.56	0.1400
40.0	716.22	0.1933	696.10	0.1669	674.44	0.1450
50.0	727.35	0.2035	708.51	0.1766	688.46	0.1543
60.0	737.37	0.2131	719.54	0.1855	700.71	0.1628
80.0	754.95	0.2306	738.63	0.2018	721.56	0.1782
100.0	770.14	0.2467	754.91	0.2165	739.07	0.1920
150.0	801.44	0.2824	787.98	0.2488	774.10	0.2217
200.0	826.67	0.3141	814.34	0.2770	801.65	0.2474
250.0	848.06	0.3434	836.53	0.3028	824.69	0.2704
300.0	866.74	0.3712	855.85	0.3269	844.66	0.2919
350.0	883.41	0.3982	873.03	0.3501	862.37	0.3123
400.0	898.51	0.4247	888.56	0.3727	878.35	0.3319
500.0	925.13	0.4775	915.89	0.4172	906.40	0.3703
600.0	948.18	0.5311	939.51	0.4619	930.61	0.4084
800.0	986.97	0.6450	979.19	0.5554	971.21	0.4871

	480		500		520	
T (K) p (MPa)	ρ/(kg m^{-3})	η/(mPa s)	ρ/(kg m^{-3})	η/(mPa s)	ρ/(kg m^{-3})	η/(mPa s)
0.01	0.080328	0.01574	0.077108	0.01642	0.074137	0.01710
0.05	0.40246	0.01573	0.38619	0.01641	0.37122	0.01709
0.10	0.80699	0.01571	0.77404	0.01640	0.74377	0.01708
0.15	1.2136	0.01570	1.1636	0.01639	1.1177	0.01707
0.20	1.6224	0.01568	1.5548	0.01638	1.4930	0.01706
0.25	2.0335	0.01567	1.9478	0.01636	1.8697	0.01705
0.30	2.4468	0.01566	2.3425	0.01635	2.2478	0.01704
0.35	2.8624	0.01564	2.7391	0.01634	2.6273	0.01704
0.40	3.2803	0.01563	3.1375	0.01633	3.0084	0.01703
0.45	3.7007	0.01561	3.5377	0.01632	3.3909	0.01702
0.50	4.1236	0.01560	3.9399	0.01631	3.7749	0.01701
0.60	4.9770	0.01557	4.7502	0.01628	4.5475	0.01699
0.80	6.7163	0.01552	6.3952	0.01624	6.1120	0.01696

TABLE 6. Viscosity and density of methanol as a function of pressure and temperature—Continued

	480		500		520	
T (K) p (MPa)	ρ/(kg m^{-3})	η/(mPa s)	ρ/(kg m^{-3})	η/(mPa s)	ρ/(kg m^{-3})	η/(mPa s)
1.00	8.5026	0.01547	8.0751	0.01620	7.7035	0.01692
1.50	13.208	0.01535	12.447	0.01611	11.811	0.01685
2.00	18.342	0.01525	17.107	0.01603	16.129	0.01679
2.50	24.049	0.01517	22.124	0.01597	20.692	0.01675
3.00	30.544	0.01512	27.581	0.01593	25.542	0.01672
3.50	38.129	0.01512	33.587	0.01593	30.727	0.01672
4.00	47.261	0.01520	40.278	0.01597	36.305	0.01675
5.00	534.55	0.07770	56.646	0.01625	48.930	0.01692
6.00	543.05	0.08033	82.778	0.01723	64.426	0.01734
8.00	556.83	0.08486	486.01	0.06441	118.74	0.02045
10.0	567.98	0.08880	510.51	0.07019	393.06	0.04823
15.0	589.61	0.09714	546.28	0.08018	488.34	0.06456
20.0	606.19	0.1042	569.60	0.08785	525.28	0.07338
25.0	619.83	0.1105	587.44	0.09440	549.95	0.08035
30.0	631.52	0.1162	602.08	0.1002	568.90	0.08637
35.0	641.80	0.1215	614.57	0.1056	584.44	0.09178
40.0	651.01	0.1265	625.51	0.1105	597.68	0.09674
50.0	667.05	0.1355	644.12	0.1195	619.56	0.1057
60.0	680.79	0.1438	659.69	0.1276	637.36	0.1136
80.0	703.71	0.1585	685.07	0.1418	665.63	0.1275
100	722.62	0.1716	705.57	0.1543	687.95	0.1396
150	759.80	0.1994	745.10	0.1807	730.05	0.1648
200	788.62	0.2231	775.27	0.2028	761.63	0.1857
250	812.54	0.2441	800.09	0.2223	787.39	0.2040
300	833.17	0.2635	821.41	0.2401	809.39	0.2205
350	851.42	0.2818	840.20	0.2567	828.73	0.2358
400	867.85	0.2993	857.09	0.2725	846.07	0.2502
500	896.64	0.3330	886.62	0.3026	876.33	0.2775
600	921.45	0.3661	912.02	0.3318	902.33	0.3037
800	962.99	0.4336	954.52	0.3908	945.77	0.3558

	540		560		580	
T (K) p (MPa)	ρ/(kg m^{-3})	η/(mPa s)	ρ/(kg m^{-3})	η/(mPa s)	ρ/(kg m^{-3})	η/(mPa s)
0.01	0.071388	0.01778	0.068836	0.01846	0.066460	0.01914
0.05	0.35738	0.01777	0.34455	0.01845	0.33262	0.01913
0.10	0.71586	0.01777	0.69003	0.01845	0.66604	0.01913
0.15	1.0755	0.01776	1.0365	0.01844	1.0003	0.01912
0.20	1.4362	0.01775	1.3838	0.01843	1.3353	0.01912
0.25	1.7981	0.01774	1.7322	0.01843	1.6712	0.01911
0.30	2.1611	0.01773	2.0815	0.01842	2.0079	0.01911
0.35	2.5254	0.01773	2.4317	0.01842	2.3454	0.01910
0.40	2.8908	0.01772	2.7830	0.01841	2.6837	0.01910
0.45	3.2574	0.01771	3.1353	0.01840	3.0230	0.01909
0.50	3.6253	0.01770	3.4886	0.01840	3.3630	0.01909
0.60	4.3647	0.01769	4.1983	0.01839	4.0458	0.01908
0.80	5.8589	0.01766	5.6303	0.01836	5.4220	0.01906
1.00	7.3746	0.01764	7.0797	0.01834	6.8127	0.01904
1.50	11.265	0.01758	10.785	0.01830	10.357	0.01901
2.00	15.314	0.01754	14.616	0.01827	14.004	0.01899
2.50	19.544	0.01751	18.586	0.01825	17.762	0.01898
3.00	23.978	0.01749	22.708	0.01824	21.639	0.01898
3.50	28.640	0.01750	26.998	0.01825	25.645	0.01900
4.00	33.558	0.01752	31.469	0.01828	29.787	0.01903
5.00	44.288	0.01766	41.016	0.01840	38.511	0.01914
6.00	56.502	0.01793	51.494	0.01862	47.880	0.01933
8.00	88.693	0.01929	76.346	0.01951	68.988	0.02002
10.0	141.04	0.02318	109.34	0.02145	94.551	0.02133
15.0	401.32	0.04955	270.16	0.03592	188.61	0.02928
20.0	469.22	0.06053	398.89	0.04946	317.84	0.04060

TABLE 6. Viscosity and density of methanol as a function of pressure and temperature—Continued

	540		560		580	
T (K) p (MPa)	ρ/(kg m^{-3})	η/(mPa s)	ρ/(kg m^{-3})	η/(mPa s)	ρ/(kg m^{-3})	η/(mPa s)
25.0	505.77	0.06814	453.60	0.05775	395.54	0.04933
30.0	531.23	0.07440	488.45	0.06423	441.28	0.05588
35.0	551.00	0.07989	513.98	0.06978	473.69	0.06139
40.0	567.27	0.08487	534.19	0.07474	498.63	0.06627
50.0	593.28	0.09373	565.30	0.08349	535.80	0.07482
60.0	613.80	0.1016	589.05	0.09118	563.26	0.08230
80.0	645.46	0.1152	624.61	0.1044	603.21	0.09519
100	669.82	0.1268	651.25	0.1158	632.35	0.1062
150	714.70	0.1511	699.14	0.1392	683.45	0.1287
200	747.76	0.1710	733.73	0.1582	719.60	0.1470
250	774.47	0.1882	761.40	0.1746	748.24	0.1627
300	797.16	0.2037	784.78	0.1893	772.29	0.1767
350	817.04	0.2180	805.19	0.2027	793.22	0.1893
400	834.82	0.2313	823.40	0.2151	811.85	0.2011
500	865.81	0.2563	855.09	0.2383	844.20	0.2227
600	892.39	0.2801	882.22	0.2601	871.87	0.2429
800	936.77	0.3268	927.51	0.3023	918.02	0.2814

	600		620		630	
T (K) p (MPa)	ρ/(kg m^{-3})	η/(mPa s)	ρ/(kg m^{-3})	η/(mPa s)	ρ/(kg m^{-3})	η/(mPa s)
0.01	0.064244	0.01981	0.062170	0.02048	0.061183	0.02081
0.05	0.32150	0.01981	0.31110	0.02048	0.30615	0.02081
0.10	0.64369	0.01980	0.62282	0.02047	0.61289	0.02081
0.15	0.96659	0.01980	0.93517	0.02047	0.92023	0.02081
0.20	1.2902	0.01979	1.2482	0.02047	1.2282	0.02080
0.25	1.6145	0.01979	1.5618	0.02047	1.5367	0.02080
0.30	1.9396	0.01979	1.8760	0.02046	1.8459	0.02080
0.35	2.2653	0.01978	2.1909	0.02046	2.1556	0.02080
0.40	2.5919	0.01978	2.5065	0.02046	2.4660	0.02079
0.45	2.9191	0.01977	2.8227	0.02045	2.7770	0.02079
0.50	3.2471	0.01977	3.1395	0.02045	3.0886	0.02079
0.60	3.9053	0.01976	3.7752	0.02045	3.7136	0.02079
0.80	5.2309	0.01975	5.0546	0.02044	4.9714	0.02078
1.00	6.5690	0.01974	6.3450	0.02043	6.2394	0.02077
1.50	9.9713	0.01972	9.6203	0.02042	9.4560	0.02076
2.00	13.460	0.01970	12.970	0.02041	12.742	0.02076
2.50	17.040	0.01970	16.396	0.02041	16.099	0.02077
3.00	20.717	0.01971	19.904	0.02043	19.532	0.02078
3.50	24.496	0.01973	23.497	0.02045	23.042	0.02081
4.00	28.382	0.01976	27.176	0.02049	26.632	0.02085
5.00	36.491	0.01987	34.804	0.02059	34.055	0.02095
6.00	45.078	0.02004	42.802	0.02076	41.808	0.02111
8.00	63.859	0.02063	59.969	0.02127	58.335	0.02160
10.0	85.361	0.02163	78.936	0.02210	76.361	0.02238
15.0	153.79	0.02678	134.84	0.02594	128.20	0.02580
20.0	251.66	0.03556	207.29	0.03249	192.28	0.03152
25.0	336.49	0.04292	286.19	0.03893	265.00	0.03757
30.0	392.73	0.04933	346.29	0.04443	325.25	0.04261
35.0	431.77	0.05468	390.69	0.04949	371.12	0.04738
40.0	461.51	0.05938	424.54	0.05396	406.66	0.05172
50.0	505.19	0.06761	474.22	0.06176	458.92	0.05929
60.0	536.72	0.07481	509.86	0.06861	496.48	0.06594
80.0	581.42	0.08724	559.49	0.08048	548.55	0.07752
100	613.25	0.09787	594.10	0.09069	584.56	0.08749
150	667.70	0.1196	652.01	0.1116	644.21	0.1080
200	705.46	0.1372	691.38	0.1285	684.39	0.1246
250	735.06	0.1523	721.93	0.1430	715.40	0.1387
300	759.77	0.1656	747.28	0.1557	741.06	0.1513
350	781.19	0.1776	769.17	0.1673	763.18	0.1625

TABLE 6. Viscosity and density of methanol as a function of pressure and temperature—Continued

T (K)	600		620		630	
p (MPa)	ρ/(kg m^{-3})	η/(mPa s)	ρ/(kg m^{-3})	η/(mPa s)	ρ/(kg m^{-3})	η/(mPa s)
400	800.23	0.1888	788.58	0.1779	782.76	0.1729
500	833.20	0.2092	822.14	0.1972	811.06	0.1917
600	861.37	0.2279	850.77	0.2148	840.11	0.2088
800	908.33	0.2634	898.48	0.2477	888.50	0.2405

350 to 600 K at pressures from 100 MPa to 10 GPa. While these conditions present formidable experimental challenges, the fundamental knowledge to be gained about the behavior of matter would certainly warrant such efforts.

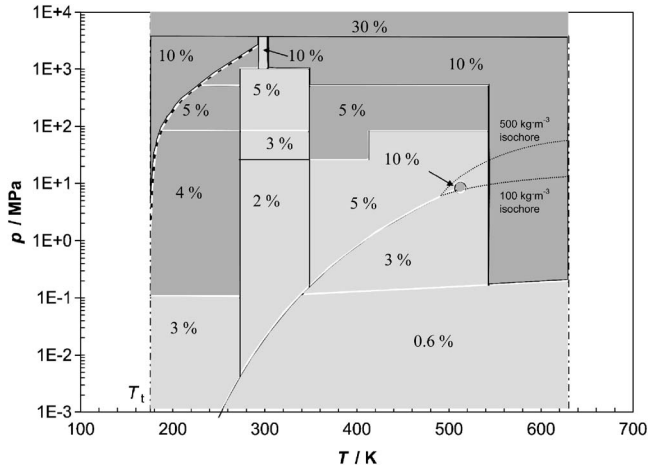

FIG. 9. Range of the viscosity representation and regions of estimated uncertainty.

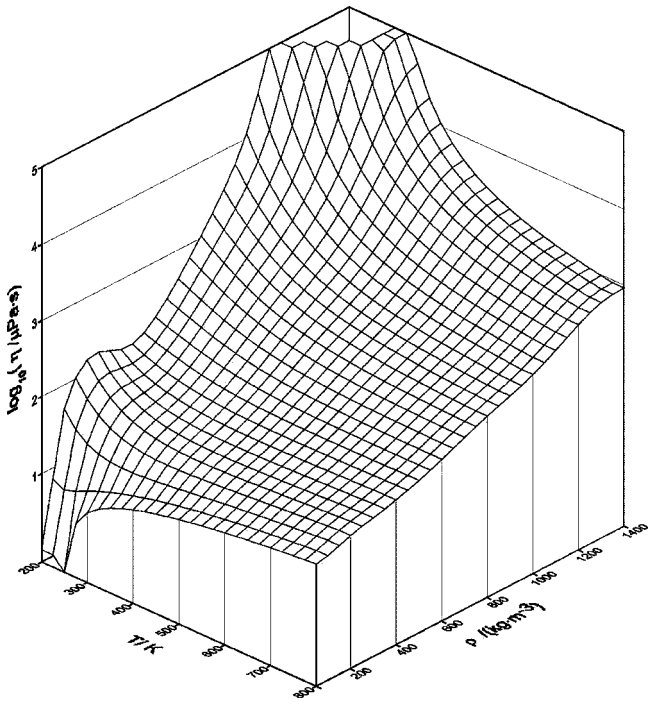

FIG. 10. Viscosity surface of methanol calculated from Eq. (18).

9. Acknowledgments

H.W.X. gratefully acknowledges the support of the K. C. Wong Education Foundation, Hong Kong, China, and of the National Institute of Standards and Technology (NIST) as a Guest Researcher for this study. We thank our NIST colleagues Daniel G. Friend, Chris Muzny, and James C. Rainwater for their valuable comments. We appreciate the comments of an anonymous journal reviewer that helped to improve the manuscript. We also thank Dr. V. Teske and Professor E. Vogel, Rostock, Germany, for kindly providing us with their manuscript prior to publication and for their assistance to obtain Russian literature for this project. Dr. Harro Bauer of Physikalisch-Technische Bundesanstalt, Braunschweig, Germany, made copies of PTB *Stoffdatenblätter* available. We are greatly indebted to Dr. Rainer Poerschke, Springer-Verlag, for CD-ROMs of the Landolt-Börnstein volumes IV/18A and B. Professor Alexander Vassermann, Odessa, Ukraine, helped us graciously to obtain Russian originals of publications by Golubev *et al.* Thanks are due to NIST guest researcher Dr. Takehiro Morioka, AIST, Japan, for translation of the paper by Mitsukuri and Tonomura in 1927. Finally, we thank our students Alicia Pope (University of Colorado at Boulder) and Justin Chichester (Colorado School of Mines) who were supported by the NIST Professional Research Experience Program (PREP).

10. References

[1] A. Allal, C. Boned, and A. Baylaucq, Phys. Rev. E **64**, 011203 (2001a).
[2] A. Allal, M. Moha-Ouchane, and C. Boned, Phys. Chem. Liq. **39**, 1 (2001b).
[3] T. M. Aminabhavi, M. I. Aralaguppi, S. B. Harogoppad, and R. H. Balundgi, J. Chem. Eng. Data **38**, 31 (1993).
[4] T. M. Aminabhavi and K. Banerjee, J. Chem. Eng. Data **43**, 509 (1998).
[5] T. M. Aminabhavi and V. B. Patil, J. Chem. Eng. Data **43**, 504 (1998).
[6] E. S. Amis, A. R. Choppin, and F. L. Padgitt, J. Am. Chem. Soc. **64**, 1207 (1942).
[7] M. J. Assael and S. K. Polimatidou, Int. J. Thermophys. **15**, 95 (1994).
[8] P. Bamelis, P. Huyskens, and E. Meeussen, J. Chim. Phys. Phys.-Chim. Biol. **62**, 158 (1965).
[9] J. Barthel, R. Neueder, and R. Meier, *Electrolyte Data Collection. Viscosity of Nonaqueous Electrolyte Solutions I: Alcohol Solutions*, Vol. 12, Pt. 3, edited by D. Behrens, R. Eckermann, and G. Kreysa (Dechema, Frankfurt am Main, 1997).
[10] E. Bich and E. Vogel, Int. J. Thermophys. **12**, 27 (1991).
[11] E. C. Bingham, G. F. White, A. Thomas, and J. L. Caldwell, Z. Phys. Chem., Stoechiom. Verwandtschaftsl. **83**, 641 (1913).
[12] C. P. Blokker, Recl. Trav. Chim. Pays-Bas **55**, 170 (1936).
[13] C. A. Boned, A. Allal, A. Baylaucq, C. K. Zéberg-Mikkelsen, D. Bessieres, and S. E. Quiñones-Cisneros, Phys. Rev. E **69**, 031203 (2004).
[14] P. W. Bridgman, Proc. Am. Acad. Arts Sci. **61**, 57 (1926).

[15] P. W. Bridgman, Proc. Am. Acad. Arts Sci. **67**, 1 (1932).
[16] P. W. Bridgman, Proc. Am. Acad. Arts Sci. **74**, 399 (1942).
[17] P. W. Bridgman, Proc. Am. Acad. Arts Sci. **77**, 115 (1949).
[18] R. S. Brokaw, Ind. Eng. Chem. Process Des. Dev. **8**, 240 (1969).
[19] T. J. Bruno and G. C. Straty, J. Res. Natl. Bur. Stand. **91**, 135 (1986).
[20] G. C. Straty, A. M. F. Palavra, and T. J. Bruno, Int. J. Thermophys. **7**, 1077 (1986).
[21] N. F. Carnahan and K. E. Starling, J. Chem. Phys. **51**, 635 (1969).
[22] L. Carrette, K. A. Friedrich, and U. Stimming, ChemPhysChem **1**, 162 (2000).
[23] S. Chapman and T. G. Cowling, *The Mathematical Theory of Nonuniform Gases*, 2nd ed. (Cambridge University Press, New York, 1952).
[24] R. L. Cook, C. A. Herbst, and H. E. King, Jr., J. Phys. Chem. **97**, 2355 (1993).
[25] A. M. Crabtree and J. F. O'Brien, J. Chem. Eng. Data **36**, 140 (1991).
[26] P. M. Craven and J. D. Lambert, Proc. R. Soc. London, Ser. A **205A**, 439 (1951).
[27] R. J. B. Craven and K. M. de Reuck, Int. J. Thermophys. **7**, 541 (1986).
[28] K. M. De Reuck and R. J. B. Craven, *International Thermodynamic Tables of the Fluid State-12. Methanol* (Blackwell, Oxford, 1993).
[29] M. Dizechi and E. Marschall, J. Chem. Eng. Data **27**, 358 (1982).
[30] K.-U. Dobberstein, G. Figurski, and W. Hintzsche, Chem. Tech. (Leipzig) **45**, 37 (1993).
[31] H. Doe, T. Kitagawa, and K. Sasabe, J. Phys. Chem. **88**, 3341 (1984).
[32] H. Doe and T. Kitagawa, Bull. Chem. Soc. Jpn. **58**, 2975 (1985).
[33] J. H. Dymond, E. Bich, E. Vogel, W. A. Wakeham, V. Vesovic, and M. J. Assael, *Dense Fluids, Transport Properties of Fluids: Their Correlation, Prediction and Estimation*, edited by J. Millat, J. H. Dymond, and C. A. N. de Castro (Cambridge University Press, Cambridge, 1996), Chap. 5.
[34] D. Enskog, K. Sven. Vetenskapsakad. Handl. **63**(4), 1 (1922).
[35] E. Fischer, Z. Phys. **127**, 49 (1949).
[36] L. R. Fokin and A. N. Kalashnikov, High Temp. **38**, 224 (2000).
[37] L. R. Fokin, V. N. Popov, and A. N. Kalashnikov, High Temp. **37**, 45 (1999).
[38] N. G. Foster and E. S. Amis, Z. Phys. Chem. (Munich) **3**, 365 (1955).
[39] N. G. Foster and E. S. Amis, Z. Phys. Chem. (Munich) **7**, 360 (1956).
[40] D. G. Friend, H. Ingham, and J. F. Ely, J. Phys. Chem. Ref. Data **20**, 275 (1991).
[41] D. G. Friend and J. C. Rainwater, Chem. Phys. Lett. **107**, 590 (1984).
[42] M. Frenkel, Q. Dong, R. C. Wilhoit, and K. R. Hall, Int. J. Thermophys. **22**, 215 (2001).
[43] B. Garcia, C. Herrera, and J. M. Leal, J. Chem. Eng. Data **36**, 269 (1991).
[44] F. H. Getman, J. Chim. Phys. Phys.-Chim. Biol. **4**, 386 (1906).
[45] R. J. Gillespie and P. L. A. Popelier, *Chemical Bonding and Molecular Geometry: From Lewis to Electron Densities* (Oxford University Press, New York, 2001).
[46] A. Z. Golik, S. D. Ravikovich, and A. V. Oritsenko, Ukr. Khim. Zh. Russ. Ed. **21**, 167 (1955), ISSN 0042–4568.
[47] I. F. Golubev and V. A. Petrov, Trudy GIAP **2**, 5 (1953), ISSN 0371–716X.
[48] I. F. Golubev, *Viscosity of Gases and Gas Mixtures: A Handbook* (Israel Program for Scientific Translations, Jerusalem, 1970).
[49] I. F. Golubev and G. G. Kovarskaya, Trudy GIAP **8**, 54 (1971), ISSN 0371–716X.
[50] I. F. Golubev and T. M. Potikhonova, Trudy GIAP **8**, 67 (1971), ISSN 0371–716X.
[51] I. F. Golubev and V. F. Likhachev, Trudy GIAP **23**, 21 (1974), ISSN 0371–716X.
[52] T. Graham, Trans. R. Soc. Edinburgh **151A**, 373 (1861), ISSN 0080–4568
[53] W. E. Grant, W. J. Darch, S. T. Bowden, and W. J. Jones, J. Phys. Chem. **52**, 1227 (1948).
[54] B. Grocholski and R. Jeanloz, J. Chem. Phys. **123**, 204503 (2005).
[55] M. Gude and A. S. Teja, J. Chem. Eng. Data **40**, 1025 (1995).
[56] L. W. Hammond, K. S. Howard, and R. A. McAllister, J. Phys. Chem. **62**, 637 (1958).
[57] A. Harlow, Ph.D. thesis, University of London, London, 1967.
[58] A. H. Harvey and A. Laesecke, Chem. Eng. Prog. **98**, 34 (2002).
[59] W. J. Hehre, L. Radom, P. v. R. Schleyer, and J. A. Pople, *Ab initio Molecular Orbital Theory* (Wiley, New York, 1986).
[60] C. A. Herbst, H. E. King, Jr., Z. Gao, and H. D. Ou-Yang, J. Appl. Phys. **72**, 838 (1992).
[61] W. Herz and G. Levi, Z. Anorg. Allg. Chem. **183**, 340 (1929).
[62] J. O. Hirschfelder, C. F. Curtiss, and R. B. Bird, *Molecular Theory of Gases and Liquids* (Wiley, New York, 1964).
[63] M. L. Huber, A. Laesecke, and R. A. Perkins, Ind. Eng. Chem. Res. **42**, 3163 (2003).
[64] O. L. Hughes and H. Hartley, Philos. Mag. **15**, 610 (1933).
[65] J. J. Hurly, K. A. Gillis, J. B. Mehl, and M. R. Moldover, Int. J. Thermophys. **24**, 1441 (2003).
[66] N. P. Isakova and L. A. Oshueva, Russ. J. Phys. Chem. **40**, 607 (1966).
[67] J. D. Isdale, A. J. Easteal, and L. A. Woolf, Int. J. Thermophys. **6**, 439 (1985).
[68] K. A. R. Ismail and M. M. Abogderah, ASME J. Sol. Energy Eng. **120**, 51 (1998).
[69] M. D. Jager, A. L. Ballard, and E. D. Sloan, Jr., Fluid Phase Equilib. **211**, 85 (2003).
[70] L. Janelli, A. K. Rakshit, and A. Sacco, Z. Naturforsch. A **29A**, 355 (1974).
[71] J. Jonas and J. A. Akai, J. Chem. Phys. **66**, 4946 (1977).
[72] S. S. Joshi, T. M. Aminabhavi, and S. S. Shukla, J. Chem. Eng. Data **35**, 187 (1990).
[73] S. S. Joshi, T. M. Aminabhavi, R. H. Balundgi, and S. S. Shukla, Indian J. Technol. **29**, 425 (1991).
[74] Kh. Khalilov, Zh. Eksp. Teor. Fiz. **9**, 335 (1939).
[75] H. Kobayashi, H. Takahashi, and Y. Hiki, Int. J. Thermophys. **16**, 577 (1995).
[76] B. I. Konobeev and V. V. Lyapin, J. Appl. Chem. USSR **43**, 806 (1970).
[77] H. Kubota, S. Tsuda, M. Murata, T. Yamamoto, Y. Tanaka, and T. Makita, Rev. Phys. Chem. Jpn. **49**, 59 (1979).
[78] A. Kumagai and C. Yokoyama, Int. J. Thermophys. **19**, 3 (1998).
[79] M. Le Berre, S. Launay, V. Sartre, and M. Lallemand, J. Micromech. Microeng. **13**, 436 (2003).
[80] T. M. Ledneva, Vestn. Mosk. Univ., Ser. Mat., Mekh., Astron., Fiz., Khim. **11**, 49 (1956).
[81] F.-M. Lee, L. E. Lahti, and C. E. Stoops, J. Chem. Eng. Data **21**, 36 (1976).
[82] P. E. Liley, T. Makita, and Y. Tanaka, *Properties of Inorganic and Organic Fluids*, edited by C. Y. Ho (Hemisphere, New York, 1988).
[83] J. J. Lindberg, Fin. Kemistsamf. Medd. **71**, 77 (1962), ISSN 0015–2498.
[84] T. D. Ling and M. van Winkle, Chem. Eng. Data Ser. **3**, 88 (1958).
[85] A. M. Martin, V. B. Rodriguez, and J. P. Jaranay, Afinidad **41**, 345 (1984), ISSN 0001–9704.
[86] F. Mato and J. L. Hernandez, An. Quim. **65**, 9 (1969).
[87] F. Mato and J. Coca, An. Quim. **68**, 17 (1971).
[88] S. Matsuo and T. Makita, Int. J. Thermophys. **12**, 459 (1991).
[89] M. S. Medani and M. A. Hasan, Can. J. Chem. Eng. **55**, 203 (1977).
[90] G. Meerlender and N. A. Aziz, Rheol. Acta **11**, 19 (1972).
[91] S. Z. Mikhail and W. R. Kimel, J. Chem. Eng. Data **6**, 533 (1961).
[92] S. Mitsukuri and T. Tonomura, J. Chem. Soc. Japan **48**, 334 (1927), ISSN 0369–4208.
[93] P. J. Mohr and B. N. Taylor, Rev. Mod. Phys. **77**, 1 (2005); see also ⟨http://physics.nist.gov/cuu/⟩
[94] L. Monchick and E. A. Mason, J. Chem. Phys. **35**, 1676 (1961).
[95] P. K. Muhuri, B. Das, and D. K. Hazra, J. Chem. Eng. Data **41**, 1473 (1996).
[96] A. Nagashima, J. Phys. Chem. Ref. Data **6**, 1133 (1977).
[97] R. D. Nelson, Jr., D. R. Lide, Jr., and A. A. Maryott, *Selected Values for Electric Dipole Moments for Molecules in the Gas Phase* (National Bureau of Standards, Washington, D.C., 1967), NSRDS-NBS 10.
[98] P. D. Neufeld, A. R. Janzen, and R. A. Aziz, J. Chem. Phys. **57**, 1100 (1972).
[99] P. S. Nikam, T. R. Mahale, and M. Hasan, J. Chem. Eng. Data **41**, 1055 (1996).
[100] P. S. Nikam, L. N. Shirsat, and M. Hasan, J. Chem. Eng. Data **43**, 732 (1998).
[101] A. K. Pal and A. K. Barua, Br. J. Appl. Phys. **1**, 71 (1968).
[102] D. Papaioannou, M. Bridakis, and C. G. Panayiotou, J. Chem. Eng. Data **38**, 370 (1993).
[103] D. Papaioannou and C. Panayiotou, J. Chem. Eng. Data **40**, 202 (1995).
[104] G. E. Papanastasiou and I. I. Ziogas, J. Chem. Eng. Data **37**, 167 (1992).
[105] H. Preston-Thomas, Metrologia **27**, 3 (1990).
[106] S. E. Quiñones-Cisneros, C. K. Zéberg-Mikkelsen, and E. H. Stenby,

Fluid Phase Equilib. **169**, 249 (2000).
[107] S. E. Quiñones-Cisneros, C. K. Zéberg-Mikkelsen, and E. H. Stenby, Fluid Phase Equilib. **178**, 1 (2001).
[108] J. C. Rainwater, J. Chem. Phys. **81**, 495 (1984).
[109] J. C. Rainwater and D. G. Friend, Phys. Rev. A **36**, 4062 (1987).
[110] M. A. Rauf, G. H. Stewart, and Farhataziz, J. Chem. Eng. Data **28**, 324 (1983).
[111] R. C. Reid and L. I. Belenyessy, J. Chem. Eng. Data **5**, 150 (1960).
[112] E. G. Richardson, Proc. R. Soc. London, Ser. A **226A**, 16 (1954).
[113] J. R. Rowley, W. V. Wilding, J. L. Oscarson, and R. L. Rowley, *DIPPR DIADEM* (Brigham Young University, Provo, Utah, 2002).
[114] R. Schneider, Dissertation, Techn. Univ. Berlin (1978).
[115] P. G. Sears, R. R. Holmes, and L. R. Dawson, J. Electrochem. Soc. **102**, 145 (1955).
[116] J. V. Sengers, Int. J. Thermophys. **6**, 203 (1985).
[117] R. B. Silgardo and J. A. Storrow, J. Soc. Chem. Ind., London **69**, 261 (1950).
[118] K. Soliman and E. Marschall, J. Chem. Eng. Data **35**, 375 (1990).
[119] K. Stephan and K. Lucas, *Viscosity of Dense Fluids* (Plenum, New York, 1979).
[120] T. Strehlow and E. Vogel, Physica A **161**, 101 (1989).
[121] Y. Tanaka, Y. Matsuda, H. Fujiwara, H. Kubota, and T. Makita, Int. J. Thermophys. **8**, 147 (1987).
[122] V. Teske and E. Vogel, J. Chem. Eng. Data **51**, 628 (2006).
[123] E. Thorpe and J. W. Rodger, Philos. Trans. R. Soc. London, Ser. A **185A**, 397 (1894).
[124] M. J. Timmermans and M. Hennaut-Roland, J. Chim. Phys. Phys.-Chim. Biol. **27**, 401 (1930).
[125] T. Titani, Bull. Chem. Soc. Jpn. **8**, 255 (1993).
[126] T. Tonomura, Sci. Rep. Tohoku Imp. Univ., Ser. 1 **22**, 104 (1933).
[127] Y. S. Touloukian, S. C. Saxena, and P. Hestermans, *Thermophysical Properties of Matter* (Plenum, New York, 1975), Vol. 11.
[128] O. F. Tower, J. Am. Chem. Soc. **38**, 833 (1916).
[129] C.-H. Tu, S.-L. Lee, and I.-H. Peng, J. Chem. Eng. Data **46**, 151 (2001).
[130] S. Uchida and K. Matsumoto, Kagaku Kogaku **22**, 570 (1958), ISSN 0375–9253.
[131] H. R. van den Berg, C. A. ten Seldam, and P. S. van der Gulik, J. Fluid Mech. **246**, 1 (1993).
[132] N. B. Vargaftik, *Tables on the Thermophysical Properties of Liquids and Gases in Normal and Dissociated States* (Hemisphere Publishing Corporation, Washington, D.C., 1975).
[133] N. B. Vargaftik, Y. K. Vinogradov, and V. S. Yargin, *Handbook of Physical Properties of Liquids and Gases: Pure Substances and Mixtures*, 3rd augmented and revised ed. (Begell House, New York, 1996).
[134] D. S. Viswanath and G. Natarajan, *Data Book on the Viscosity of Liquids* (Hemisphere, New York, 1989).
[135] E. Vogel, E. Bich, and R. Nimz, Physica A **139A**, 188 (1986).
[136] E. Vogel, C. Küchenmeister, E. Bich, and A. Laesecke, J. Phys. Chem. Ref. Data **27**, 947 (1998).
[137] E. Vogel, J. Wilhelm, C. Küchenmeister, and M. Jaeschke, High Temp. - High Press. **32**, 73 (2000).
[138] W. Weber, Rheol. Acta **14**, 1012 (1975).
[139] L. Werblan, Bull. Acad. Pol. Sci. Ser. Sci. Chim. **27**, 903 (1979), ISSN 0001–4095.
[140] R. Whorton and E. S. Amis, Z. Phys. Chem. (Munich) **8**, 9 (1956).
[141] J. Wilhelm and E. Vogel, Int. J. Thermophys. **21**, 301 (2000).
[142] Ch. Wohlfarth and B. Wohlfarth, *Viscosity of Pure Organic Liquids and Binary Liquid Mixtures*, Subvolume B. Pure Organic Liquids, edited by M. D. Lechner and W. Martienssen, Landolt-Börnstein-Numerical Data and Function Relationships in Science and Technology, IV/18 (Springer, Berlin, 2001).
[143] C. L. Yaws, *Physical Properties* (McGraw–Hill, New York, 1977).
[144] T. W. Yergovich, G. W. Swift, and F. Kurata, J. Chem. Eng. Data **16**, 222 (1971).
[145] J. M. Zaug, L. J. Slutsky, and J. M. Brown, J. Phys. Chem. **98**, 6008 (1994).
[146] C. K. Zéberg-Mikkelsen, A. Baylaucq, G. Watson, and C. Boned, Int. J. Thermophys. **26**, 1289 (2005).
[147] V. N. Zubarev, P. G. Prusakov, and L. V. Sergeeva, *Thermophysical Properties of Methanol. A Handbook* (Izdat. Standartov, Moscow, 1973) (in Russian).